Engineering and Technology Journal e-ISSN: 2456-3358

Volume 09 Issue 07 July-2024, Page No.- 4462-4483

DOI: 10.47191/etj/v9i07.18, I.F. – 8.227

© 2024, ETJ

Characterizing Mesophase Transitions of 8CB Liquid Crystal using DSC and Logger Pro

William LeBrun[1], Dipti Sharma (PhD)[2]

[1]Undergraduate student, Emmanuel College Boston, MA, 02115 USA

[2]Supervisor, Emmanuel College, Boston, MA 02115 USA

ABSTRACT: The main focus of this research is to perform a detailed analysis of 4-octyl-4-cyanobiphenyl (8CB) Liquid Crystal (LC). 8CB is a family member of the nCB liquid crystal and it is a thermotropic LC that shows a change in phase transition when it is heated or cooled. The phase transitions for 8CB occur in four phases, including a crystalline (K), Smectic A (SmA), Nematic (N), and Isotropic (I) state. As 8CB goes through these states, it shows mesophases and mesophase transitions. 8CB has a tail made of eight C-H bonds and a body made of two benzene and CN groups. Further, this paper presents findings derived from the utilization of Differential Scanning Calorimetry (DSC) and explores the thermal characteristics of 8CB when subjected to heating from 0°C to 100°C and subsequent cooling from 100°C to -40°C, using ramp rates of 5, 10, and 20 °C/min respectively. This paper also includes results that can be found in this study when thermal Speed, thermal acceleration, and thermal Jerk are calculated using Logger Pro for 8CB against the time taken for these mesophase transitions. It can be seen how the peaks of these mesophases change as a function of thermal speed, thermal acceleration, and thermal jerk. These results can be explained in terms of molecular alignment and effect of temperature on their mesophases and the flexibility of 8CB's tail.

KEYWORD: Physics, Chemistry, Crystalline, Smectic A, Nematic, Isotropic, Liquid Crystal (LCs), Liquid Crystal Display, 8CB, Phase Change, Heating, Cooling, Temperature, Heat Flow, Specific Heat Capacity, Temperature, Endothermic, Exothermic, LoggerPro, Data, Material Science.

INTRODUCTION

Liquid Crystals (LCs) are generally a state of matter that exhibit properties of both liquids and crystalline solids. The molecules in liquid crystals are found in a regular long-ranged arrangement but are not necessarily fixed in one position like a solid crystal. Liquid crystals can be found in the phases of a solid crystalline state, Smectic C, Smectic A, Nematic, and finally an isotropic state. The reason why we are interested in thermotropic LCs is the possible applications they could be used in. LCs can have differing physical properties depending on their state, changing their optical, mechanical, and electrical properties. A result of this is a large array of possible uses and versatility with this material, including the current use of LCs in television screens and even the future possible use in nanotechnology. [1-3]

To understand the behavior of LCs, it is important to understand their phase transitions (mesophases). Phase change or phase transition is the process in which there is a transformation of the physical properties of matter as it changes its thermodynamic phase. In our case, this change is initiated by heating up or cooling down 8CB. For this research, we used a thermal technique called Differential Scanning Calorimetry (DSC) to detect these phase and temperature changes. During a phase change, DSC shows a change in heat flow with temperature and time and that is a phase change detected in LCs using DSC. [4] Typically, this can be seen in a phase change diagram comparing Temperature and Heat Energy added to the system.

Differential Scanning Calorimetry (DSC) is an instrument that uses its own technique to measure the heat flow of the material as a function of temperature or time which detects phase transitions in the liquid crystals being sampled. These DSC machines produce data points that can then be interpreted as graphs based on the position, intensity, and shape of the peaks. These peaks reveal information about how the LC being tested changed and the phases it went through during the heating and cooling cycles. Different states and phases of LCs can be detected easily using DSC. [5]

One state that is particularly interesting and useful for applications using 8CB is the Nematic state. The nematic state in a LC is a phase that is represented by the molecular arrangement known as nematic order. This order has the molecules stay parallel to each other, but still have the capability to slide by one another, leading to a semi-liquid crystalline state. Nematic LCs are important to the current technological world as they are the most common type of LC used in LCDs or liquid crystal displays that can be found in television screens and certain optical devices. The nematic

state is especially sought after due to its relatively stable structure while also having fluidity and the ability to flow. [6-7]

A LCD or liquid crystal display is a form of display that uses a layer of liquid crystals sandwiched between two transparent electrodes. This setup allows for the precise control of the properties of liquid crystals, allowing images to be shown by controlling the intensity and amount of light. The details of how LCs work in LCDs can be seen here. When light enters the LCD panel, it passes through a polarizing filter. This polarized light then encounters the liquid crystal layer. When no voltage is applied, the liquid crystal molecules align themselves parallel to each other due to their inherent properties. When a voltage is applied across the electrodes, an electric field is created within the liquid crystal layer. This electric field affects the orientation of the liquid crystal molecules. By selectively applying voltages to different areas of the liquid crystal layer, individual pixels on the display can be activated or deactivated, controlling the passage of light and creating the desired image. Today, the vast majority of contemporary commercial LCDs rely on more advanced versions of this basic concept, using either twisted nematic (TN) or super-twisted nematic (STN) technology. [8-9]

For a long time, there was more than one type of liquid crystal used in practical applications such as 8CB and 5CB, both of which have been used in LCDs. This study is more interested in 8CB as it is easily available and can be manufactured quickly. The 8CB is called 4-Cyano-4'-octylbiphenyl and is an example of a thermotropic LC with 8 carbons in its alkyl chain and a molecular formula of C21H25N. 8CB is a molecule made up of a biphenol group, a cyano group, and a carbon tail made up of 8 carbons. 8CB has a solid crystalline phase, a smectic phase, a nematic phase, and finally an isotropic phase. It is one of the most versatile and used liquid crystals in manufacturing and technology. [10-11]

LCD's 8CB is a commonly used liquid crystal due to the fact its Smectic and Nematic phases occur at room temperature, meaning no special cooling or heating is required to keep the crystals in the smectic phase. In addition to this, 8CB has a density that is close to water and a relatively high viscosity for a liquid crystal. Although his viscosity is dependent on temperature. Liquid crystals that have these specific characteristics of room temperature smectic phase and high viscosity such as 8CB can form sub-micrometer thick films. Sub-micrometer thick films are sought after in various fields such as nanotechnology, optics, electronics, and materials science including LCDs. Their thinness allows for precise control over properties like electrical conductivity, optical transparency, and surface interactions. [12]

To understand the detailed behavior of LCs, especially to better understand the characteristics of 8CB phases, we decided to use Logger Pro as an analysis tool. The Logger Pro is a data collection and analysis software developed by Vernier Software & Technology, and specially used in colleges for labs. Logger Pro provides tools that can be used to analyze any data further in detail such as plotting graphs, performing statistical analysis, and generating mathematical models to interpret experimental results. [13] Being a college student, I believe Logger Pro has been very useful for data analysis and has performed reliably, even when performing analysis using large quantities of data, which is why I decided to use it to analyze the 8CB results obtained by DSC.

METHODS

Octyl Cyanobiphenyl (8CB), a thermotropic liquid crystal from the nCB family, was used for the study. Its chemical name is 4-octyl-4-cyanobiphenyl (8CB). A bulk sample of 8CB was taken to study its thermal behavior using the Differential Scanning Calorimetry (DSC) technique, provided by WPI, Worcester, MA, USA.

The molecular weight of 8CB is given as 291.43 g/mol. [14] A small amount of 19.1 mg of 8CB was taken and then sealed in DSC's pan and lid for further study. This sealed pan and lid were then placed into a DSC instrument, model DSC 214 instrument from the NETZSCH company that is at WPI's chemistry and biochemistry department. The sample of 8CB was then run from -40 °C to 100 °C and then back from 100 °C to -40 °C with three different 5 °C/min, 10 °C/min, and 20 °C/min ramp rates. The DSC instrument gave DSC thermograms with data for heat flow versus time and temperature. The collected data was then taken to Logger Pro for further detailed analysis of phase transitions of 8CB.

The 8CB molecule has two benzene rings in the body of the molecule, one CN group at the head of the body, and eight C-H groups in its tail. The shape of 8CB is like a rod or a worm with a tail. The diagram of the 8CB molecule is shown in **Figure 1 and Figure 2.** A table showing the typical molecular arrangement of liquid crystals showing all mesophases can be seen in **Figure 3** and a table showing the molecular arrangement for 8CB specifically is shown in **Figure 4.**

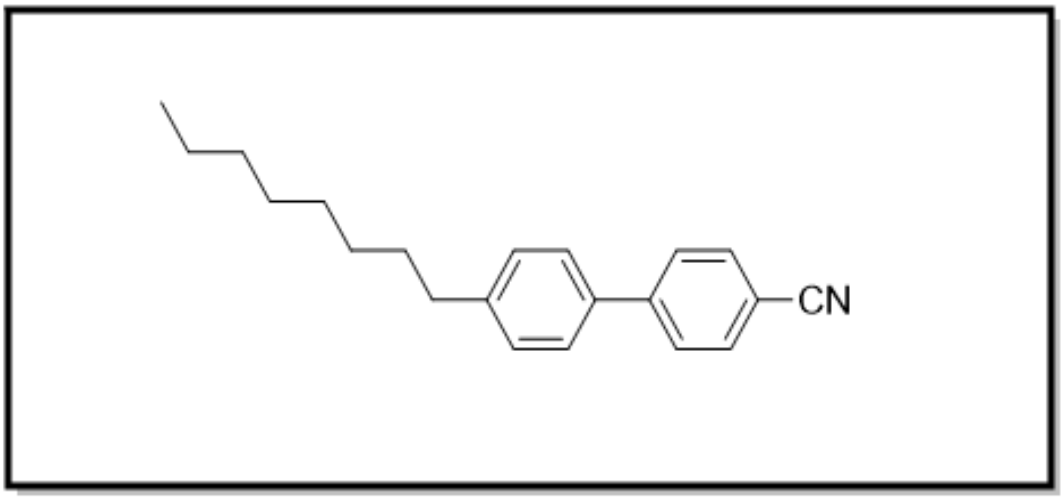

Figure 1: Cartoon of 8CB liquid crystal molecule.

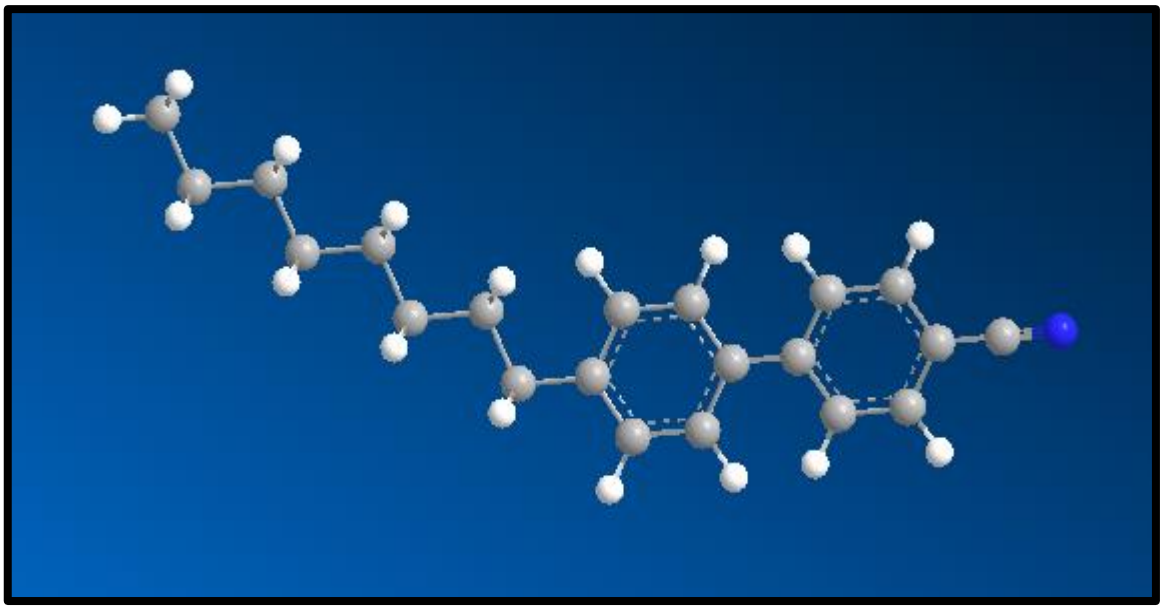

Figure 2: 3D Cartoon of 8CB liquid crystal molecule.

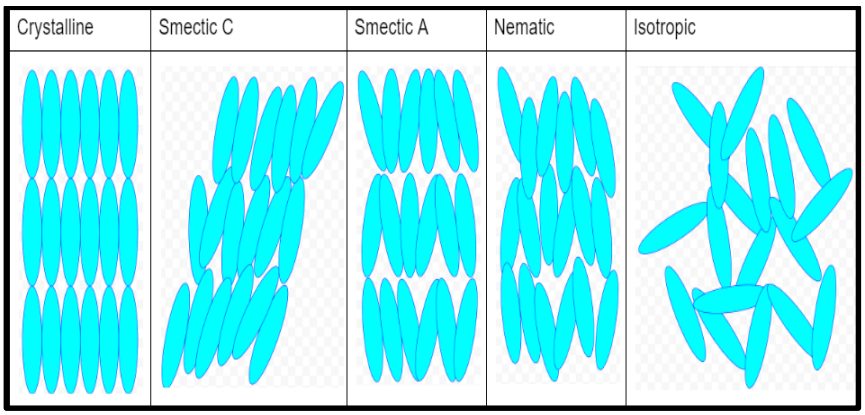

Figure 3: Typical Molecular arrangement of liquid crystals showing mesophases. From left to right, it shows Crystalline, Smectic C, Smectic A, Nematic, and Isotropic.

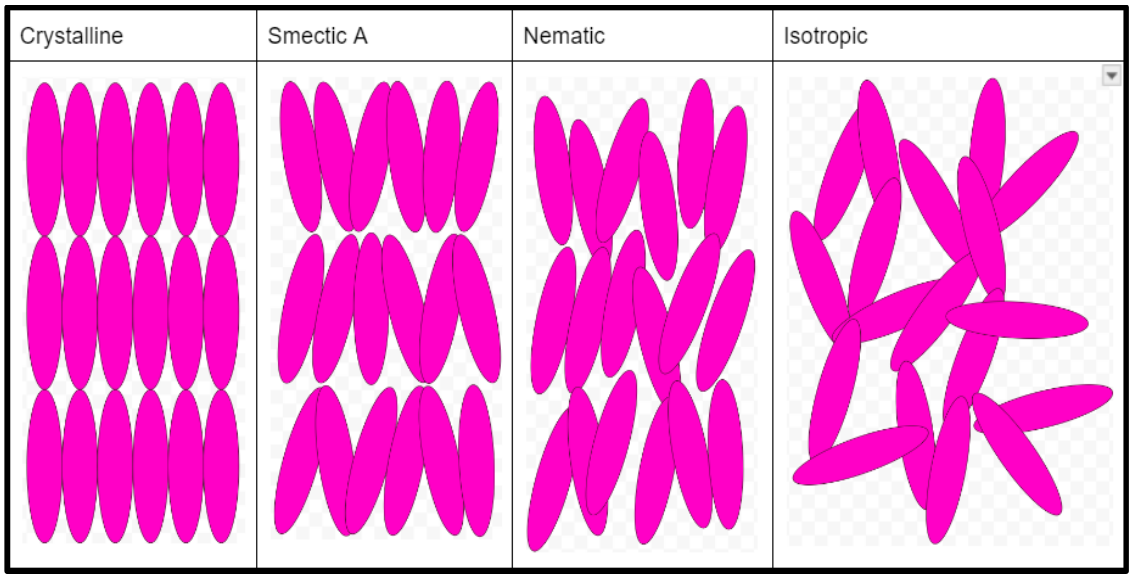

Figure 4: Molecular arrangement of 8CB liquid crystal showing mesophases. From left to right, it shows Crystalline, Smectic A, Nematic, and Isotropic. [15]

THEORY

This study follows thermodynamics. The sample of 8CB was studied using a DSC instrument which is based on how heat flows in the sample with time and temperature change. Following a change in heat flow with time and temperature, the following theory can be given.

When a sample is heated in DSC, thermal energy in the form of heat goes in and the temperature of the sample changes, and some features appear in DSC curves if any phase transitions take place. According to thermodynamics, the heat (Q) is given by equation 1. In this equation, m is the mass of the sample, Cp is the specific heat capacity of the sample, and $\boldsymbol{\Delta T}$ is the change in temperature of the sample in Kelvin. The flow of heat which is also called heat flow (dQ/dt) and heating rate (dT/dt) can be seen in equation 2.

$$\boldsymbol{Q = m * Cp * \Delta T} \qquad -1$$

$$\boldsymbol{\frac{dQ}{dT} = m * Cp * \frac{dT}{dt}} \qquad -2$$

The heat flow (HF) can also be written as shown in equation 3.

$$HF = m * Cp * \frac{dT}{dt} = \frac{dQ}{dt} \qquad -3$$

Now, we will take derivatives of HF. The first derivative of the HF gives the thermal speed (v) shown in Equation 4, that gives the change in heat flow with a given time ($\frac{d(HF)}{dt}$).

$$v = \frac{d(HF)}{dt} = m * Cp * \frac{d^2(Q)}{dt^2} \qquad -4$$

The second derivative of the heat flow equation gives the Thermal acceleration (a) shown in equation 5.

$$a = \frac{d(v)}{dt} = m * Cp * \frac{d^3(Q)}{dt^3} \qquad -5$$

$$J = \frac{d(a)}{dt} = m * C * \frac{d^4(Q)}{dt^4} \qquad -6$$

In a similar way, the third derivative of the heat flow equation gives the thermal jerk (J), shown in equation 6.

We are applying all these theories to 8CB data obtained from DSC for three different ramp rates and the results are shown in the result section.

RESULTS

This section is a collection of the data results that were analyzed during this experiment. It includes Heat Flow vs Time, incorporating metrics such as speed, acceleration, and jerk derived from this graph. Additionally, it presents graphs depicting Heat Flow vs Temperature. Detailed information regarding peak Temperature and observed times for three mesophases of 8CB, including the 1st, 2nd, and 3rd derivatives for heating at rates of 5, 10, and 20 °C/min, can be found in **Tables 1-7**.

Graphs illustrating Heat Flow vs Time and Temperature, alongside Thermal speed, acceleration, and jerk at a heating ramp rate of 5 °C/min, are presented in **Figures 5-9**. Corresponding graphs for a cooling ramp rate of 5 °C/min can be found in **Figures 10-14**. Similarly, for a heating ramp rate of 10 °C/min, refer to **Figures 15-19**, and for cooling at the same rate, **Figures 20-24**. Graphs for a heating ramp rate of 20 °C/min are displayed in **Figures 25-29**, and for cooling at this rate, in **Figures 30-34**. Moreover, **Figures 35 and 36** showcase Heat Flow vs Time graphs with all cumulative data

.

Table 1: Temperature of Peaks observed in Heating / Cooling process for 8CB.

Rate °C/min	Cycle	Tk (°C) of peak	Tsm(°C) of peak	Tn (°C) of peak
5	Heating	27.56	36.18	42.63
	Cooling	-4.6	40.5	96.4
10	Heating	29.3	37.76	44.2
	Cooling	-8.1	39.9	92.5
20	Heating	33.0	35.8	45.0
	Cooling	-8.5	37.9	86.2

Table 2. Peak Temperature and times observed for three mesophases of 8CB for 1st, 2nd, and 3rd derivatives for heating with 5°C/min rate.

Derivative	t_k1 (min)	HF_k1 (mW/mg)	t_k2 (min)	HF_k2 (mW/mg)	t_sm (min)	HF_ksm (mW/mg)	t_n1(min)	HF_n1 (mW/mg)	t_n2 (min)	HF_n1 (mW/mg)
1st ((mW/mg)/min)	2.09	9.83	6.24	1.95	6.92	-4.05	9.47	1.15	9.74	-3.90
2nd ((mW/mg/min^2)	2.07	155	6.81	-21.6	6.97	22.1	9.36	12.1	9.54	-18.4
3rd ((mW/mg/min^3)	2.11	2890	6.47	552	6.83	-194	9.33	340	9.71	-561

Table 3. Peak Temperature and times observed for three mesophases of 8CB for 1st, 2nd, and 3rd derivatives for cooling with 5°C/min rate.

Derivative	t_k1 (min)	HF_k1 (mW/mg)	t_k2 (min)	HF_k2 (mW/mg)	t_sm (min)	HF_ksm (mW/mg)	t_n1(min)	HF_n1 (mW/mg)	t_n2 (min)	HF_n1 (mW/mg)
1st ((mW/mg)/min)	22.26	-0.59	33.77	-1.08	34.01	0.63	42.72	-22.73	42.98	12.94
2nd ((mW/mg/min^2)	22.15	-8.3	33.53	-23.6	33.58	26.8	42.68	-260.3	42.92	318.4
3rd ((mW/mg/min^3)	22.06	-228	33.54	-961	33.57	1565	42.92	-6651	42.74	7602

Table 4. Peak Temperature and times observed for three mesophases of 8CB for 1st, 2nd, and 3rd derivatives for heating with 10°C/min rate.

Derivative	t_k1 (min)	HF_k1 (mW/mg)	t_k2 (min)	HF_k2 (mW/mg)	t_sm (min)	HF_ksm (mW/mg)	t_n1(min)	HF_n1 (mW/mg)	t_n2 (min)	HF_n1 (mW/mg)
1st ((mW/mg)/min)	53.63	1.37	57.74	3.95	58.36	-4.78	59.32	1.40	59.46	-0.95
2nd ((mW/mg/min^2)	53.40	12.1	57.42	12.3	57.98	-56.5	59.27	32.5	59.43	-52.1
3rd ((mW/mg/min^3)	53.32	519	57.97	2823	57.90	-1164	59.41	2130	59.42	-3792

Table 5. Peak Temperature and times observed for three mesophases of 8CB for 1st, 2nd, and 3rd derivatives for cooling with 10°C/min rate.

Derivative	t_k1 (min)	HF_k1 (mW/mg)	t_k2 (min)	HF_k2 (mW/mg)	t_sm (min)	HF_ksm (mW/mg)	t_n1(min)	HF_n1 (mW/mg)	t_n2 (min)	HF_n1 (mW/mg)
1st ((mW/mg)/min)	66.28	-1.02	71.93	-1.82	72.14	0.72	76.50	-15.26	76.78	8.14
2nd ((mW/mg/min^2)	66.12	-13.1	71.86	-88.7	71.87	40.4	76.47	-144.3	76.66	246.7
3rd ((mW/mg/min^3)	66.41	505	71.84	-5899	71.86	7332	76.64	-6825	76.66	5442

Table 6. Peak Temperature and times observed for three mesophases of 8CB for 1st, 2nd, and 3rd derivatives for heating with 20°C/min rate.

Derivative	t_k1 (min)	HF_k1 (mW/mg)	t_k2 (min)	HF_k2 (mW/mg)	t_sm (min)	HF_ksm (mW/mg)	t_n1 (min)	HF_n1 (mW/mg)	t_n2 (min)	HF_n1 (mW/mg)
1st ((mW/mg)/min)	82.86	2.23	84.54	9.21	84.98	-7.28	85.29	1.40	85.38	-2.40
2nd ((mW/mg/min^2)	82.64	26.5	84.32	63.3	84.67	-158.5	85.26	106.5	85.32	-115.7

3rd ((mW/mg/min^3)	**82.87**	**3230**	**84.31**	**3202**	**84.66**	**-4549**	**85.30**	**7954**	**85.31**	**-13686**

Table 7. Peak Temperature and times observed for three mesophases of 8CB for 1st, 2nd, and 3rd derivatives for cooling with 20°C/min rate.

Derivative	t_k1 (min)	HF_k1 (mW/mg)	t_k2 (min)	HF_k2 (mW/mg)	t_sm (min)	HF_ksm (mW/mg)	t_n1(min)	HF_n1 (mW/mg)	t_n2 (min)	HF_n1 (mW/mg)
1st ((mW/mg)/min)	**89.30**	**-2.04**	**92.01**	**-3.79**	**92.17**	**0.89**	**94.76**	**-21.84**	**94.96**	**17.45**
2nd ((mW/mg/min^2)	**89.12**	**-25.3**	**91.98**	**-154.9**	**92.04**	**100.7**	**94.74**	**-172.9**	**94.91**	**481.4**
3rd ((mW/mg/min^3)	**89.62**	**-3774**	**91.97**	**-17846**	**92.02**	**13865**	**94.91**	**-18627**	**94.88**	**17041**

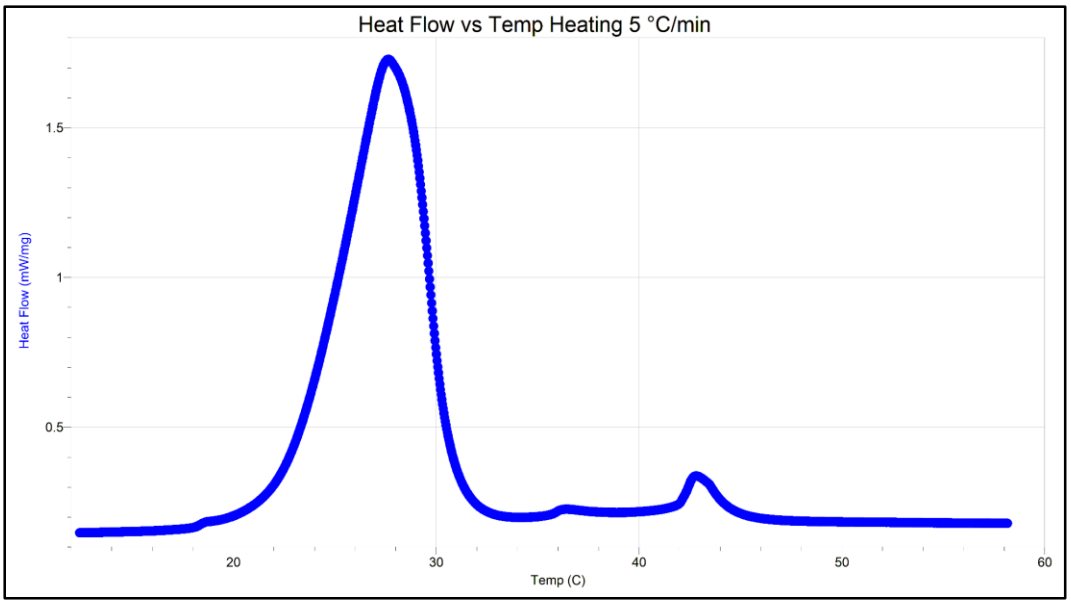

Figure 5: Heat flow vs temp graph for 8CB liquid crystal while it is heating in DSC with 5 °C/min rate.

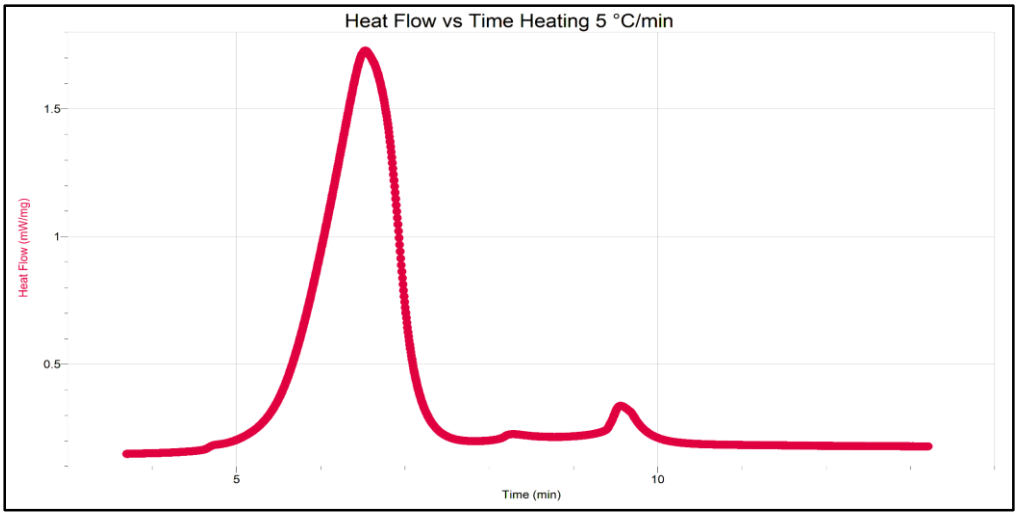

Figure 6: Heat flow vs time graph for 8CB liquid crystal while it is heating in DSC with 5 °C/min rate.

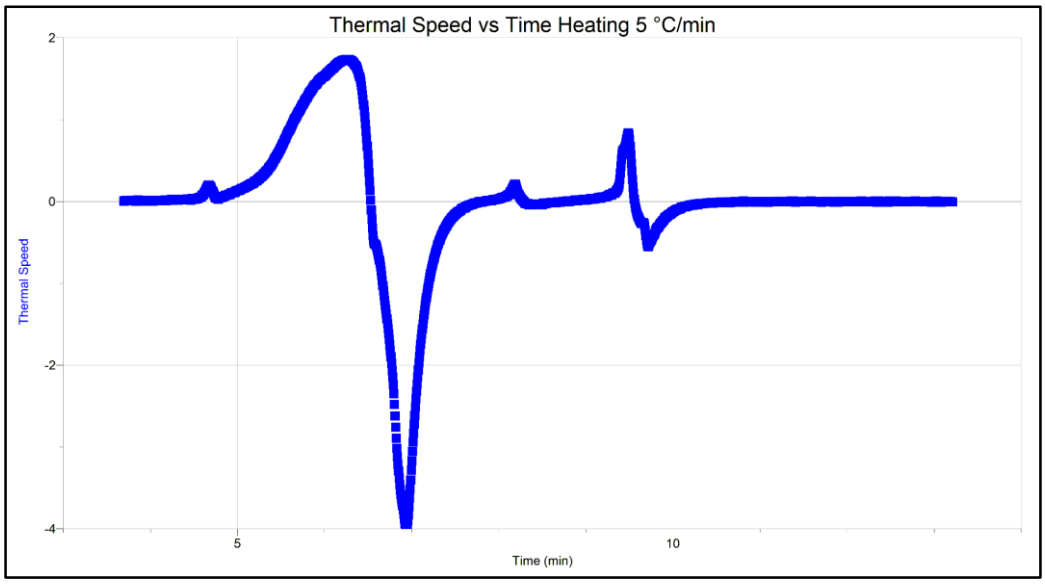

Figure 7: Thermal speed vs time graph for 8CB liquid crystal while it is heating in DSC with 5 °C/min rate.

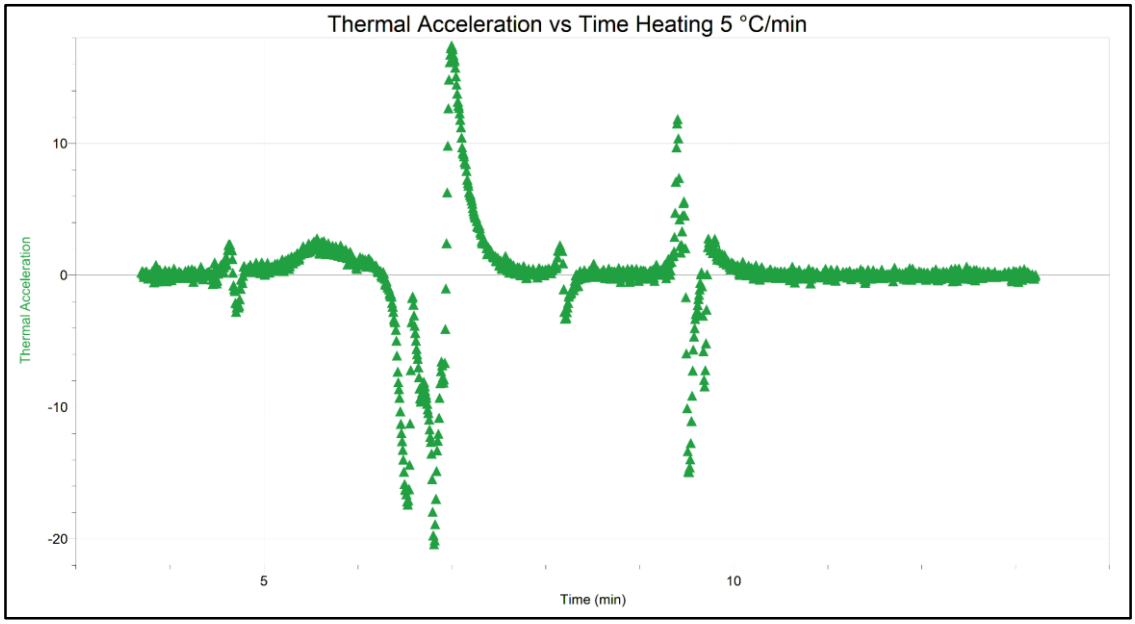

Figure 8: Thermal acceleration vs time graph for 8CB liquid crystal while it is heating in DSC with 5 °C/min rate.

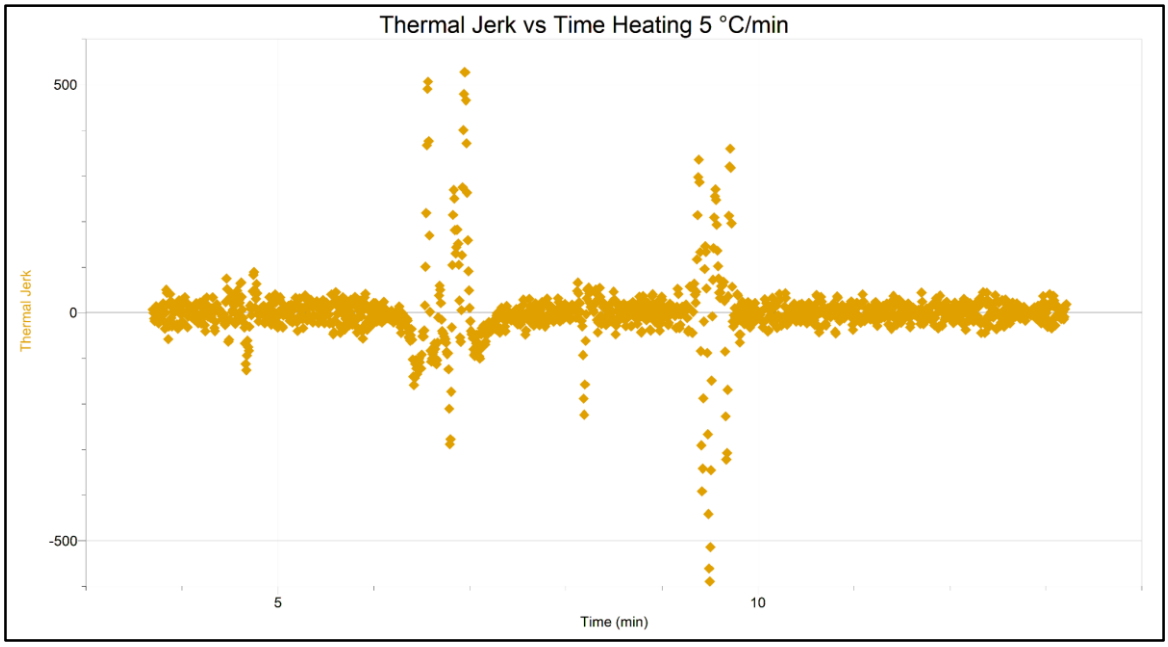

Figure 9: Thermal jerk vs time graph for 8CB liquid crystal while it is heating in DSC with 5 °C/min rate.

Figures 5-9 depict the data collected for the ramp rate of (0°C/5.0(K/min)/100°C). **Figure 5** presents a comparison between temperature and heat flow for the phase peak, with detailed data available in **Table 1.** In **Figure 6**, the heat flow and time are illustrated for the heating process of 8CB LC, showcasing peaks corresponding to crystalline (k), smectic (sm), and nematic (n) phases. **Figures 7-9** offer comparisons of heat flow and time, utilizing quantitative representations of thermal speed, acceleration, and jerk. **Equations 4-6** were used to create these derived graphical representations through LoggerPro. The peak values for the derivative graphs are documented in **Table 2**.

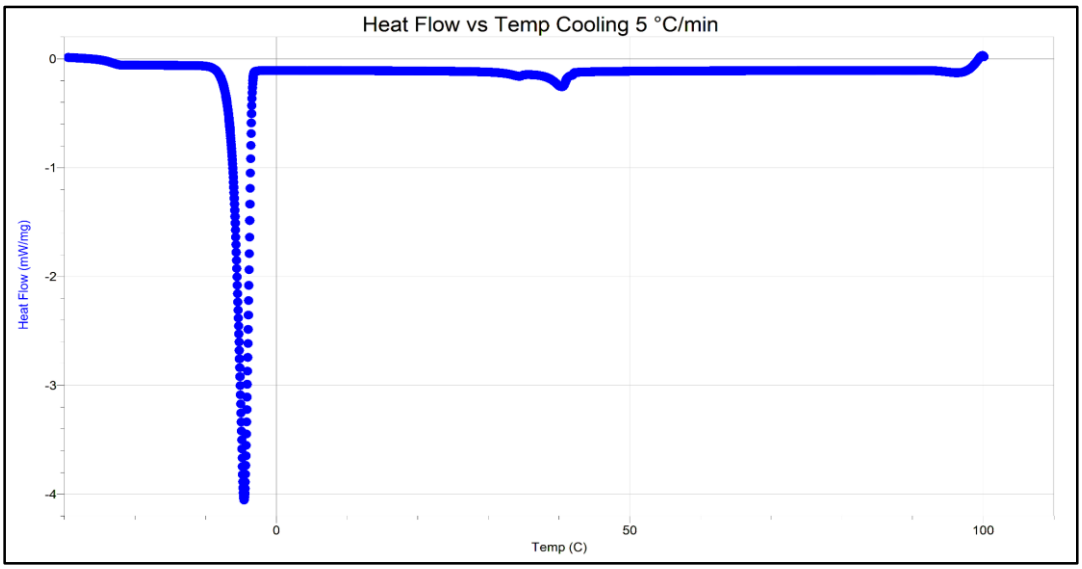

Figure 10: Heat flow vs temp graph for 8CB liquid crystal while it is cooling in DSC with 5 °C/min rate.

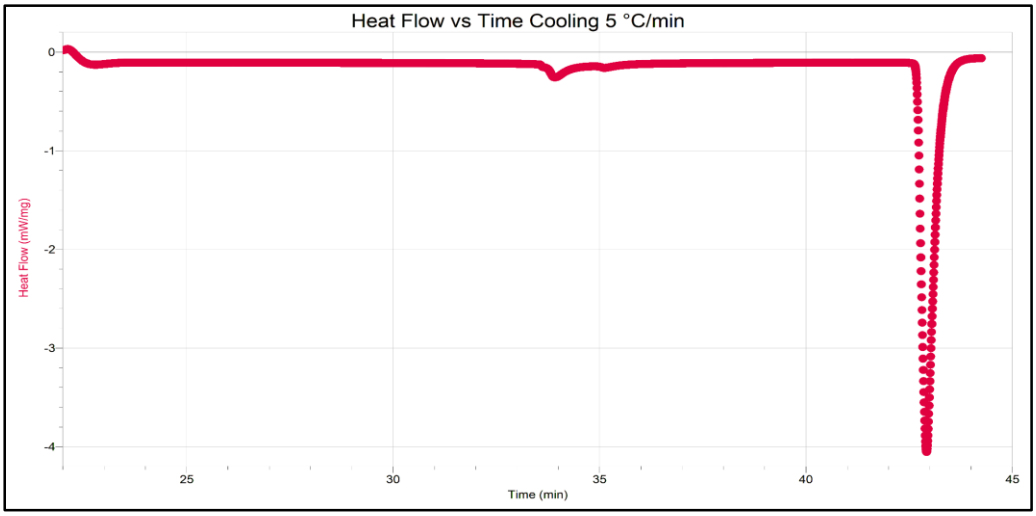

Figure 11: Heat flow vs time graph for 8CB liquid crystal while it is cooling in DSC with 5 °C/min rate.

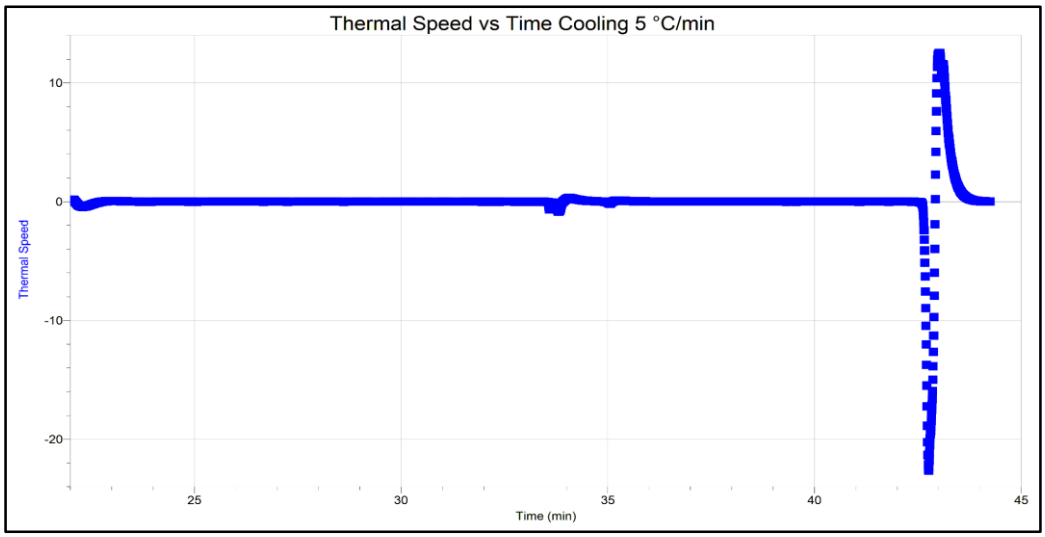

Figure 12: Thermal speed vs time graph for 8CB liquid crystal while it is cooling in DSC with 5 °C/min rate.

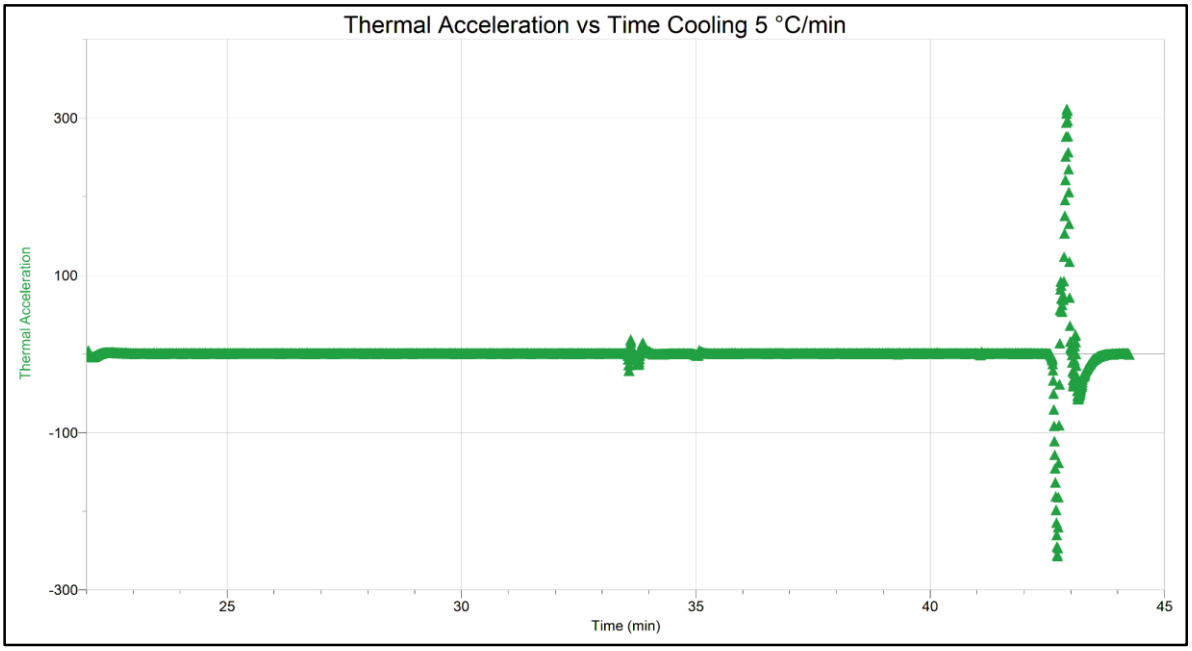

Figure 13: Thermal acceleration vs time graph for 8CB liquid crystal while it is cooling in DSC with 5 °C/min rate.

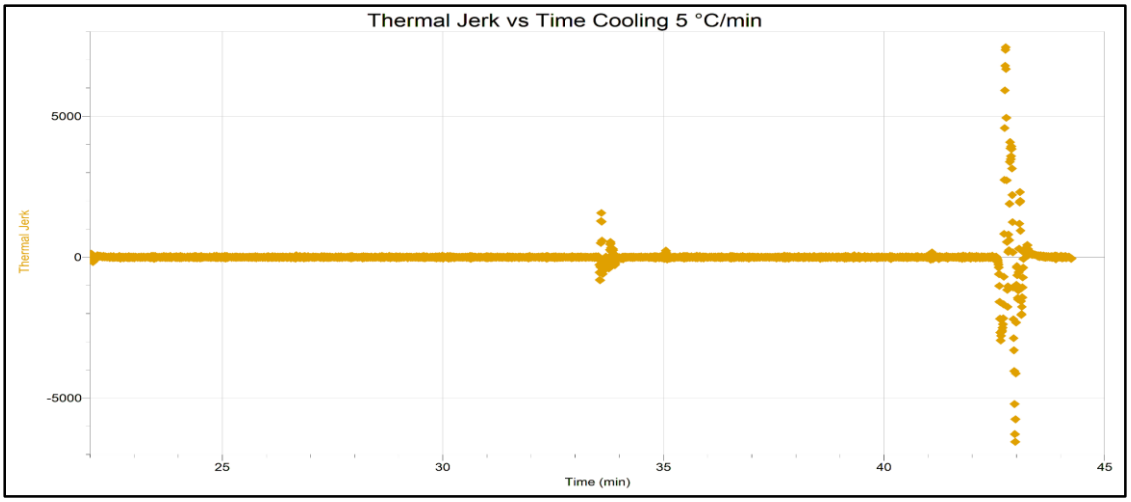

Figure 14: Thermal jerk vs time graph for 8CB liquid crystal while it is cooling in DSC with 5 °C/min rate.

Figures 10-14 depict the data gathered for the ramp rate of (0°C/10.0(K/min)/100°C). **Figure 10** presents a comparison between temperature and heat flow for the phase peak, with detailed data provided in **Table 3.** In **Figure 11**, the heat flow and time during the cooling of 8CB LC are displayed, featuring peaks corresponding to crystalline (k), smectic (sm), and nematic (n) phases. **Figures 7-9** offer comparisons of heat flow and time, utilizing quantitative representations of thermal speed, acceleration, and jerk. **Equations 4-6** were utilized to generate these derived graphical representations using LoggerPro. The peak values for the derivative graphs are documented in **Table 3.**

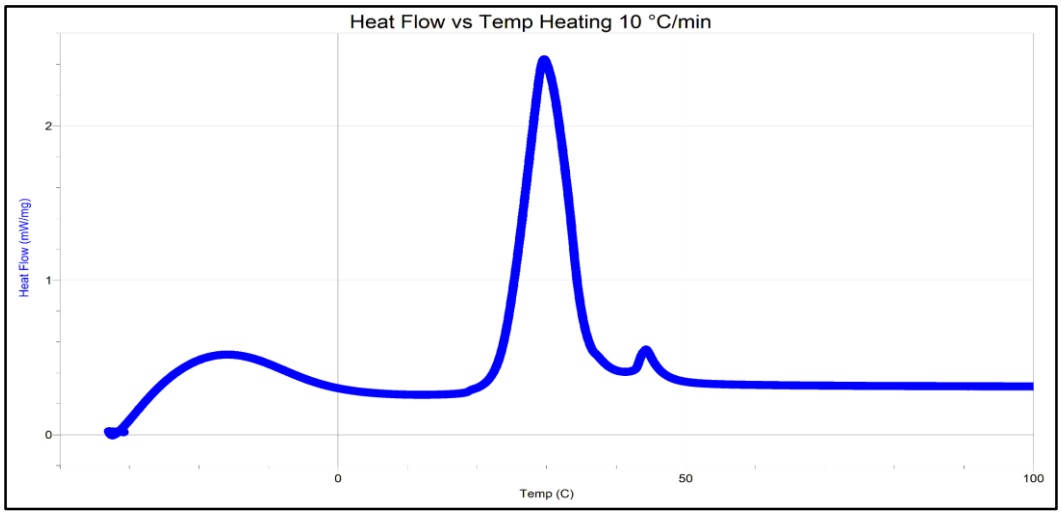

Figure 15: Heat flow vs temp graph for 8CB liquid crystal while it is heating in DSC with 10 °C/min rate.

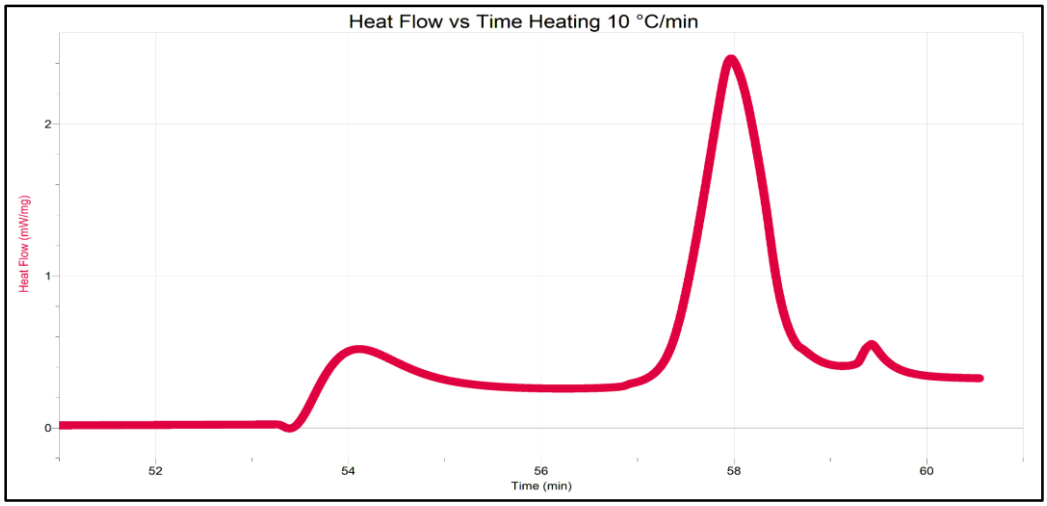

Figure 16: Heat flow vs time graph for 8CB liquid crystal while it is heating in DSC with 10 °C/min rate.

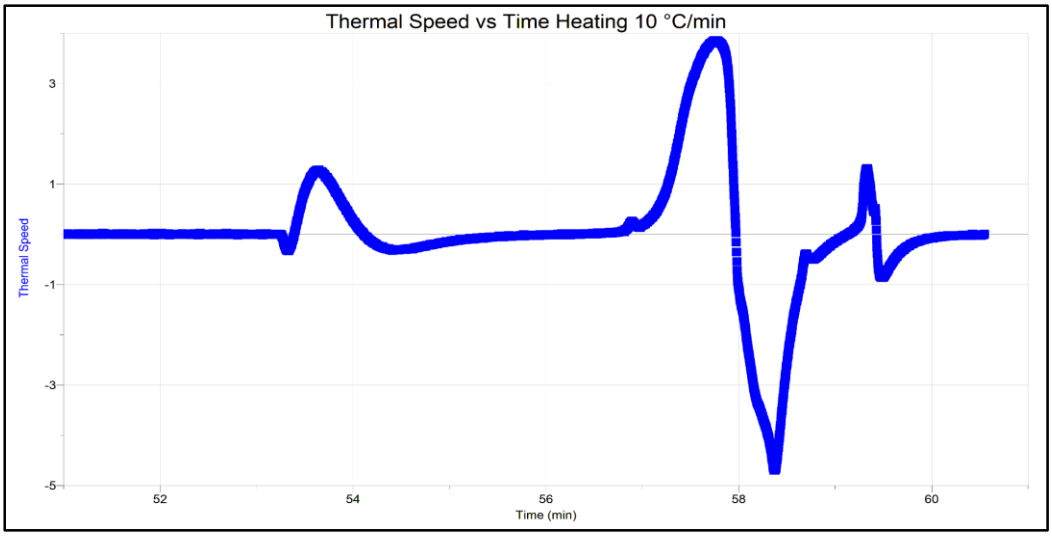

Figure 17: Thermal speed vs time graph for 8CB liquid crystal while it is heating in DSC with 10 °C/min rate.

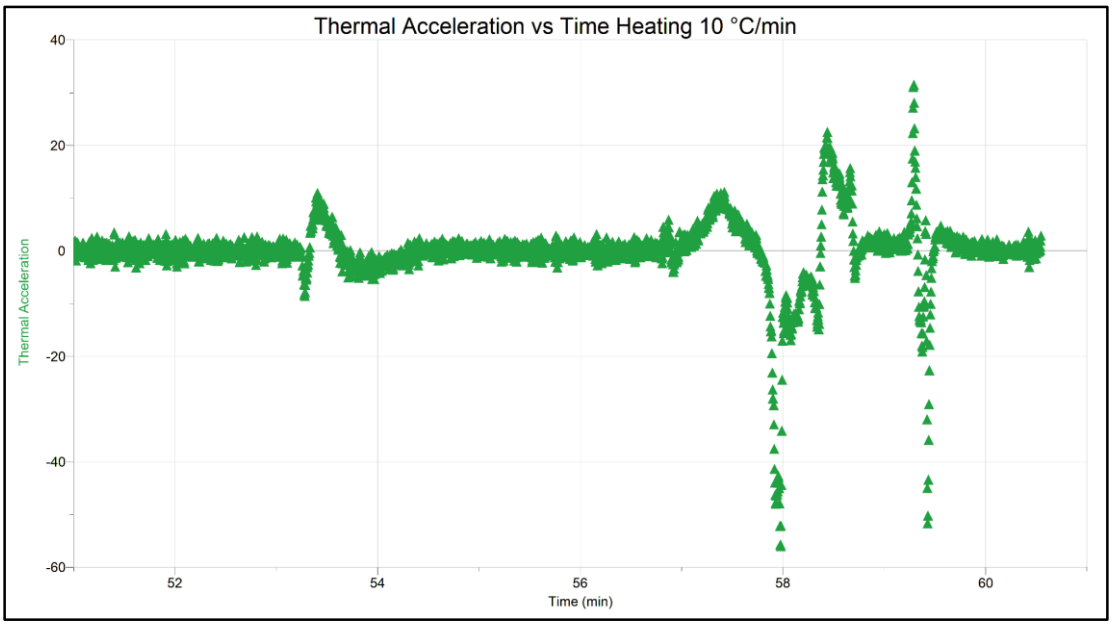

Figure 18: Thermal acceleration vs time graph for 8CB liquid crystal while it is heating in DSC with 10 °C/min rate.

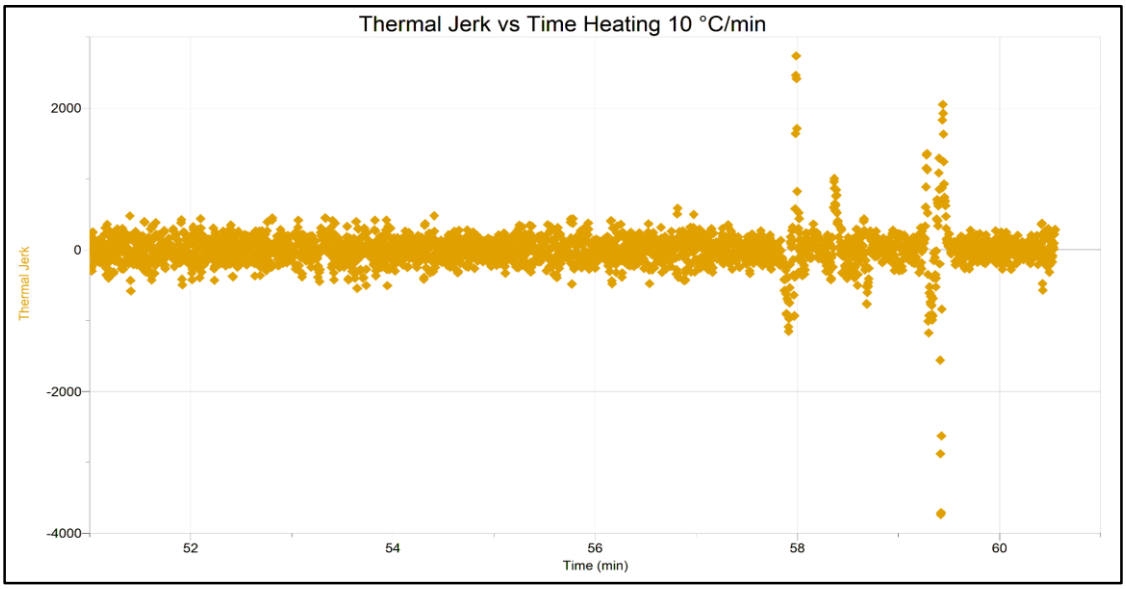

Figure 19: Thermal jerk vs time graph for 8CB liquid crystal while it is heating in DSC with 10 °C/min rate.

Figures 15-19 depict the data gathered for the ramp rate of (0°C/10.0(K/min)/100°C). **Figure 15** offers a comparison between temperature and heat flow for the phase peak, with detailed data provided in **Table 1**. In **Figure 16**, the heat flow and time are illustrated for the heating process of 8CB, displaying peaks corresponding to crystalline (k), smectic (sm), and nematic (n) phases. **Figures 17-19** present comparisons of heat flow and time, utilizing quantitative representations of thermal speed, acceleration, and jerk. **Equations 4-6** were utilized to create these derived graphical representations using LoggerPro. The peak values for the derivative graphs are documented in **Table 4.** Due to the heightened heat flow, the time taken for the 8CB peak transition from k_1 to n_2 was 5.83 minutes, compared to the initial run of 5.0(K/min) which occurred over 7.65 minutes.

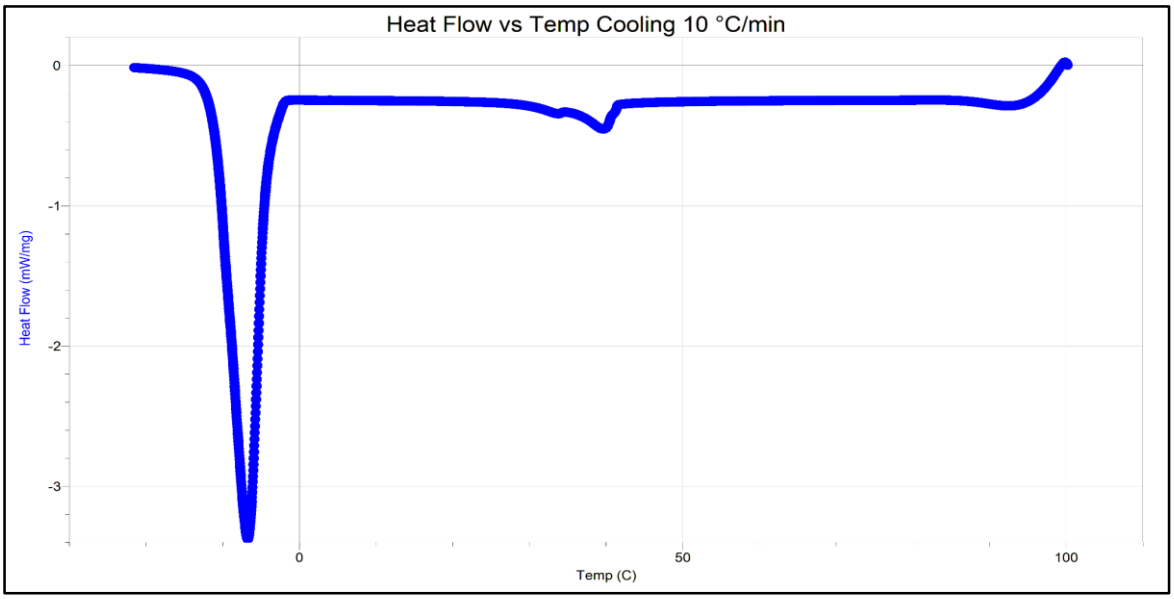

Figure 20: Heat flow vs temp graph for 8CB liquid crystal while it is cooling in DSC with 10 °C/min rate.

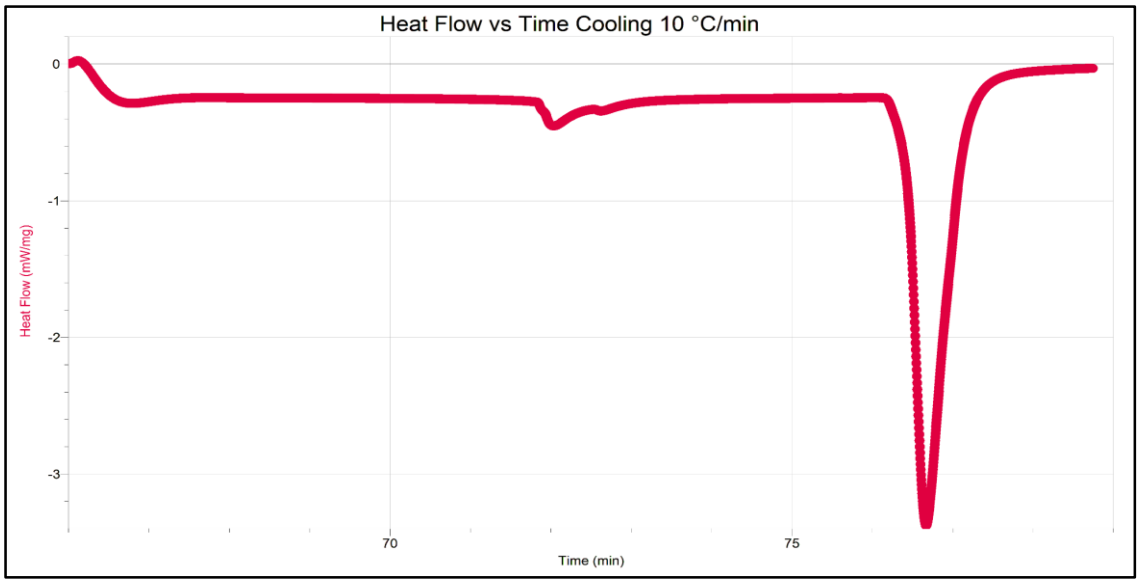

Figure 21: Heat flow vs time graph for 8CB liquid crystal while it is cooling in DSC with 10 °C/min rate.

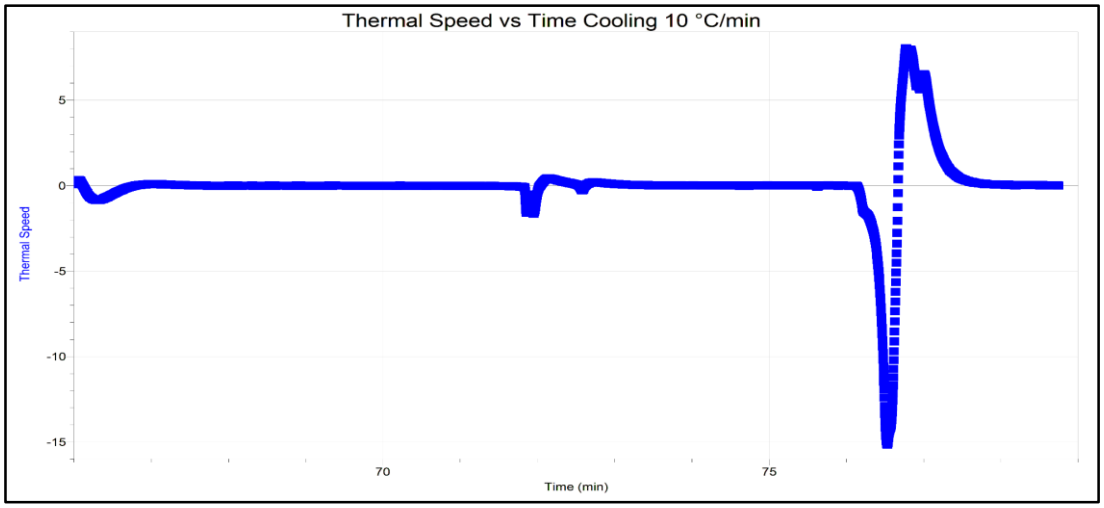

Figure 22: Thermal speed vs time graph for 8CB liquid crystal while it is cooling in DSC with 10 °C/min rate.

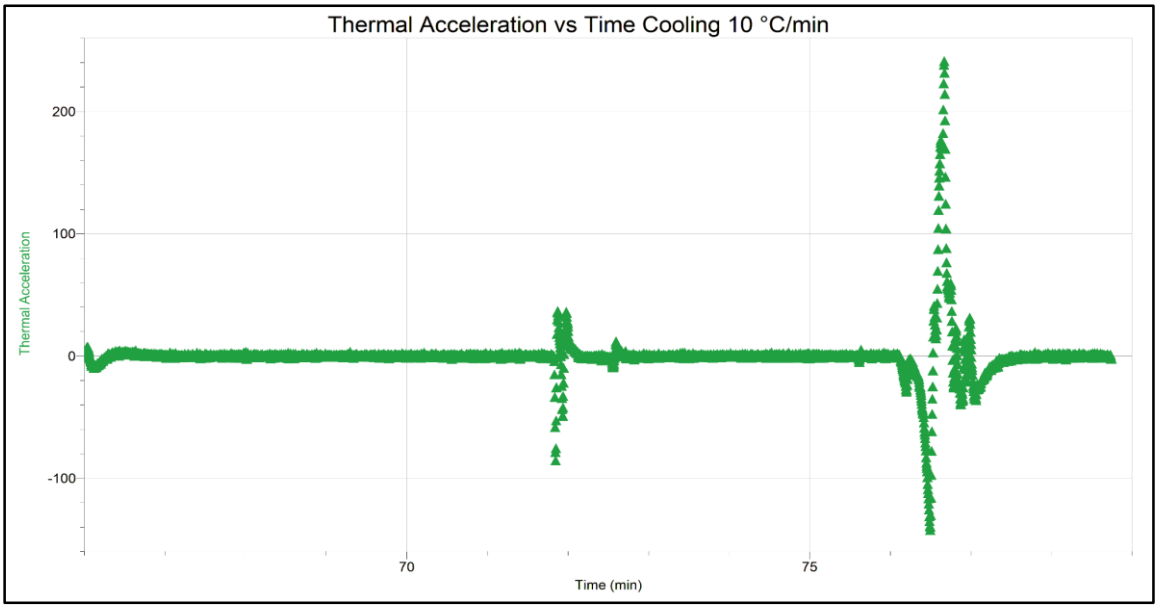

Figure 23: Thermal acceleration vs time graph for 8CB liquid crystal while it is cooling in DSC with 10 °C/min rate.

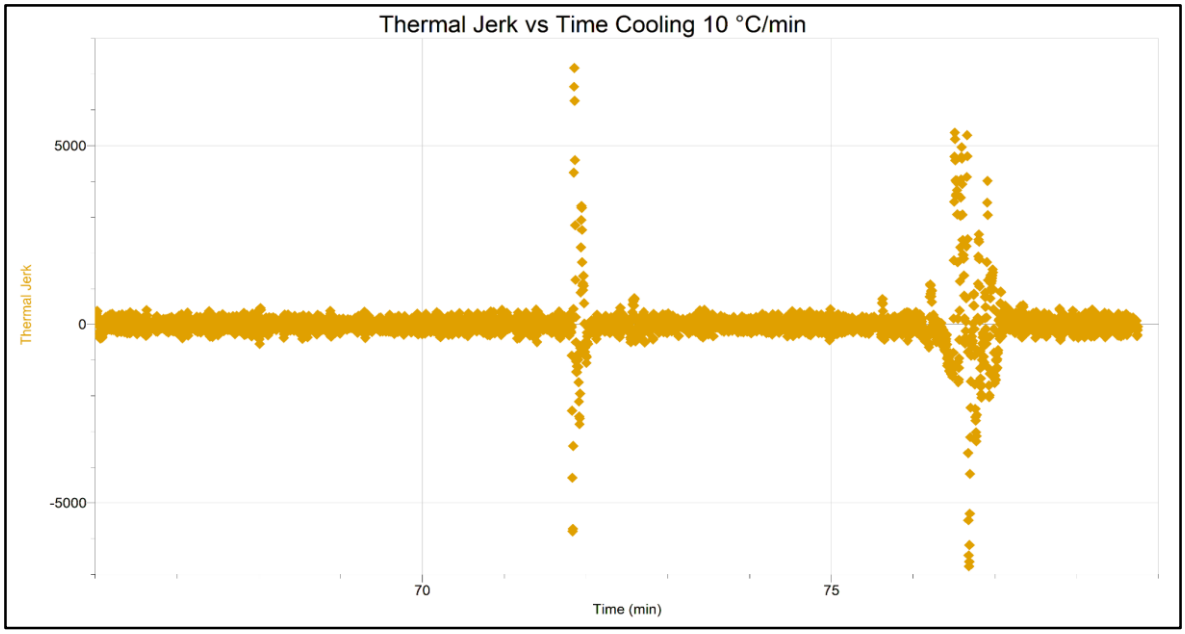

Figure 24: Thermal Jerk vs time graph for 8CB liquid crystal while it is cooling in DSC with 10 °C/min rate.

Figures 20-24 illustrate the data collected for the ramp rate of (0°C/10.0(K/min)/100°C). **Figure 20** presents a comparison between temperature and heat flow for the phase peak, with detailed data provided in **Table 3.** In **Figure 21**, the heat flow and time during the cooling of 8CB LC are depicted, featuring peaks corresponding to crystalline (k), smectic (sm), and nematic (n) phases. **Figures 22-24** offer comparisons of heat flow and time, utilizing quantitative representations of thermal speed, acceleration, and jerk. **Equations 4-6** were utilized to generate these derived graphical representations using LoggerPro. The peak values for the derivative graphs are documented in **Table 5**. Additionally, a similar relationship observed in the ramp rate of 10°C/min heating, compared to the ramp rate of 5°C/min heating, is apparent in the segment ramp rate of 10°C/min cooling when compared to the ramp rate of 5°C/min cooling. Despite the relatively similar temperatures at which phase changes occurred, the change in heat flow and particle movement has been significantly amplified with the increased flow rate of 10.0(K/min).

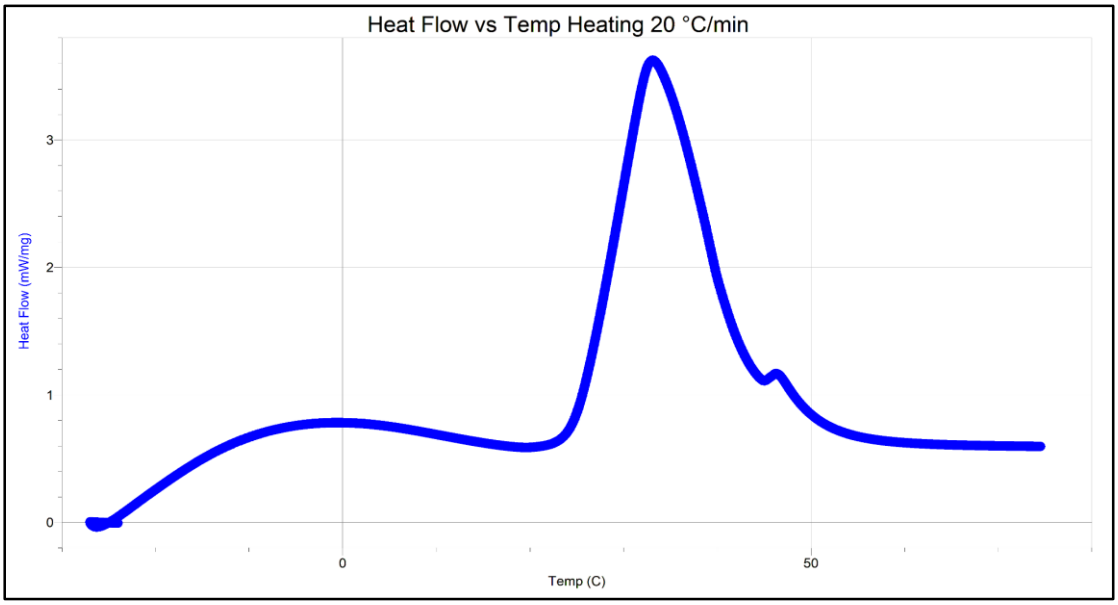

Figure 25: Heat flow vs temp graph for 8CB liquid crystal while it is heating in DSC with 20 °C/min rate.

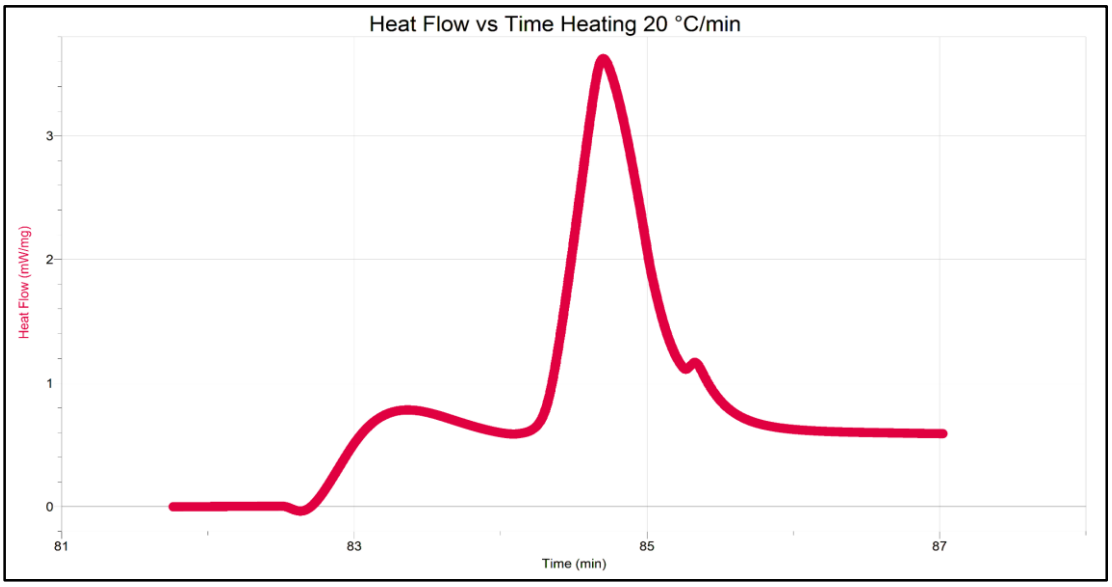

Figure 26: Heat flow vs time graph for 8CB liquid crystal while it is heating in DSC with 20 °C/min rate.

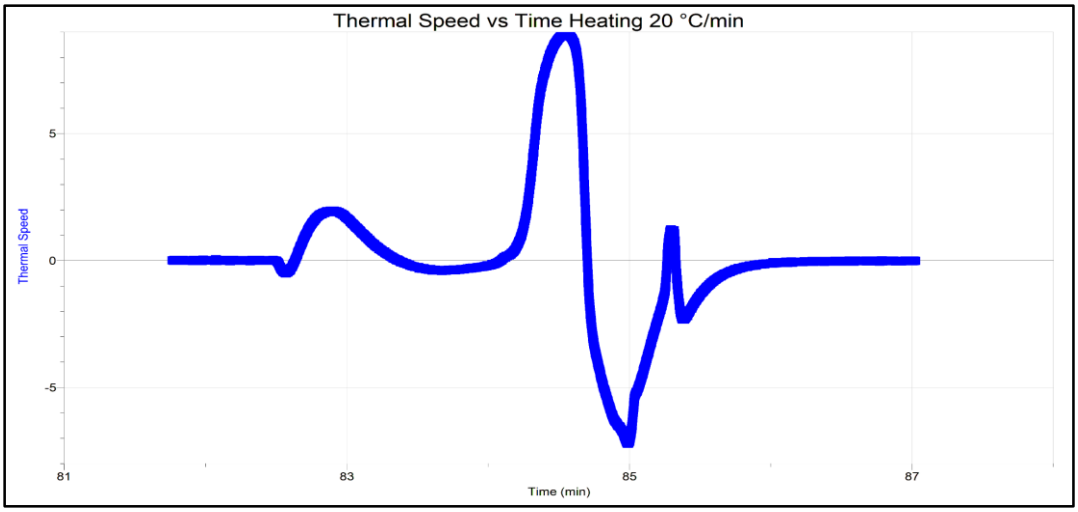

Figure 27: Thermal speed vs time graph for 8CB liquid crystal while it is heating in DSC with 20 °C/min rate.

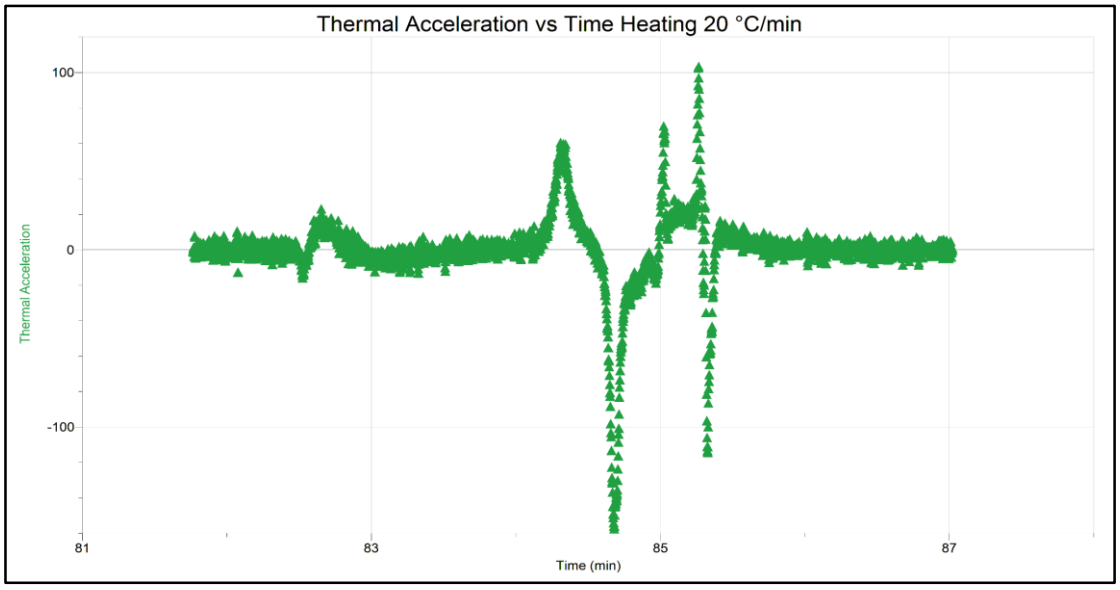

Figure 28: Thermal acceleration vs time graph for 8CB liquid crystal while it is heating in DSC with 20 °C/min rate.

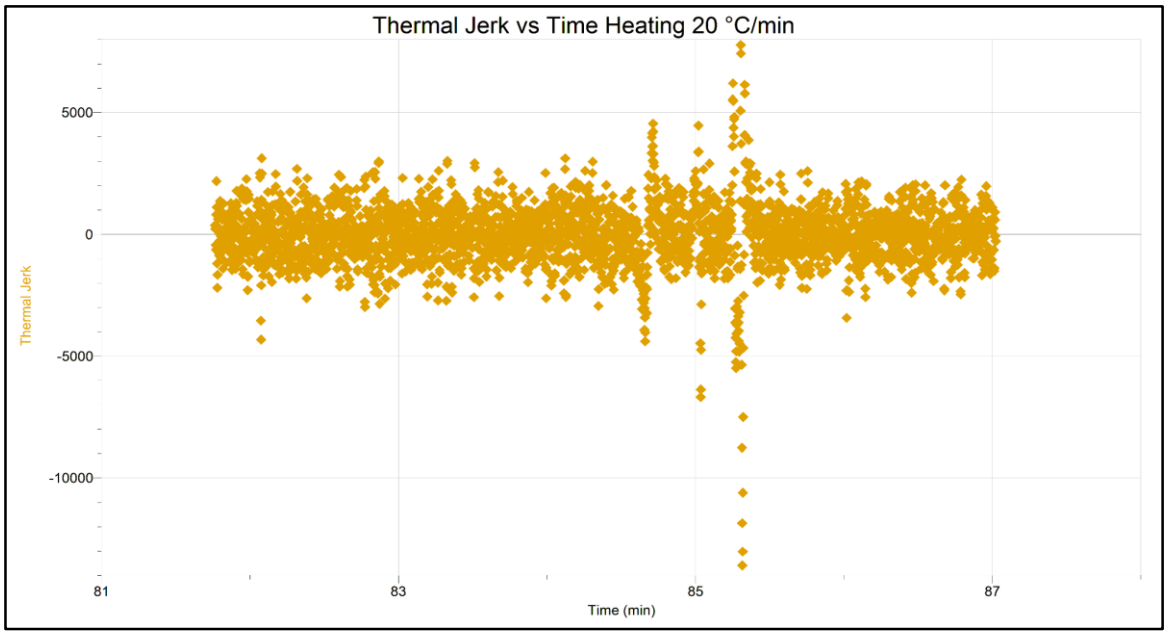

Figure 29: Thermal Jerk vs time graph for 8CB liquid crystal while it is heating in DSC with 20 °C/min rate.

Figures 25-29 portray the data collected for the ramp rate of (0°C/20.0(K/min)/100°C). **Figure 25** offers a comparison between temperature and heat flow for the phase peak, with detailed data provided in **Table 1.** In **Figure 26**, the heat flow and time during the heating of 8CB LC are depicted, highlighting peaks for crystalline (k), smectic (sm), and nematic (n) phases. **Figures 27-29** present comparisons of heat flow and time, utilizing quantitative representations of thermal speed, acceleration, and jerk. **Equations 4-6** were employed to generate these derived graphical representations using LoggerPro. The peak values for the derivative graphs are documented in **Table 6.** Additionally, the phenomenon observed in the ramp rate of 10°C heating also manifests in the ramp rate of 20°C/min heating, as evidenced by **Figure 26**, showcasing the effects of increased heat flow rates. This is further supported by the absorbance of the smectic peak into the crystalline transition peak, as depicted in **Figure 25**. Due to the heightened heat flow, the time taken for the 8CB peak transition from k_1 to n_2 was 2.52 minutes, compared to the other run of 10.0(K/min) which occurred over 5.83 minutes.

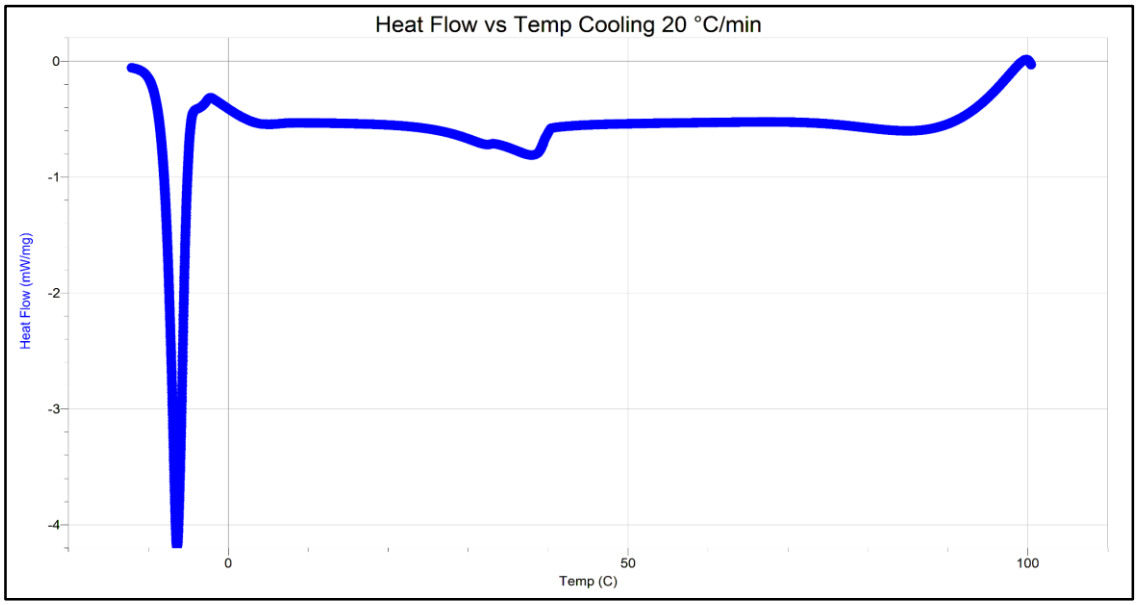

Figure 30: Heat flow vs temp graph for 8CB liquid crystal while it is cooling in DSC with 20 °C/min rate.

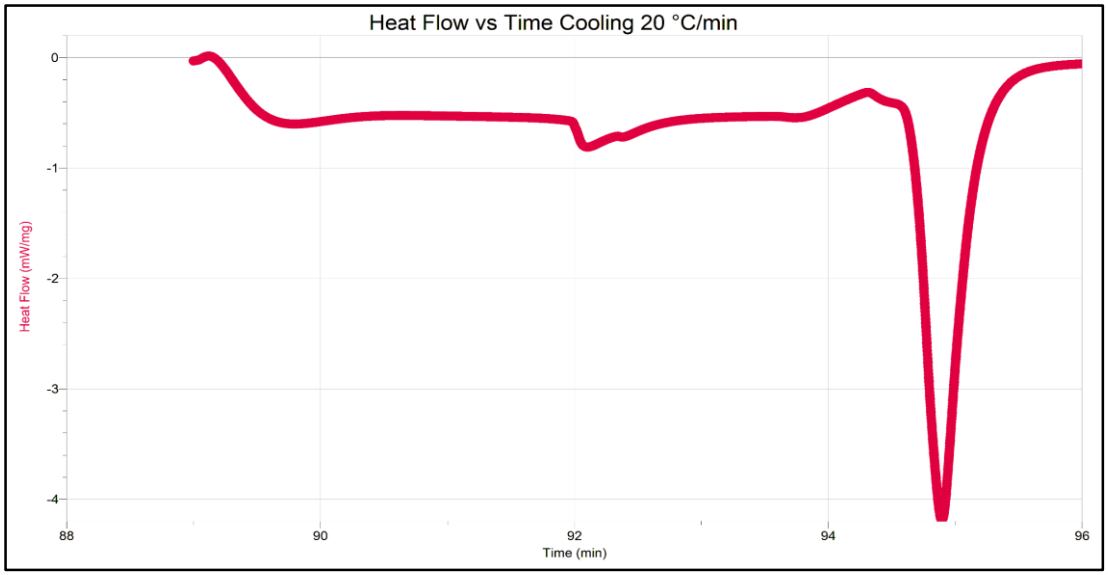

Figure 31: Heat flow vs time graph for 8CB liquid crystal while it is cooling in DSC with 20 °C/min rate.

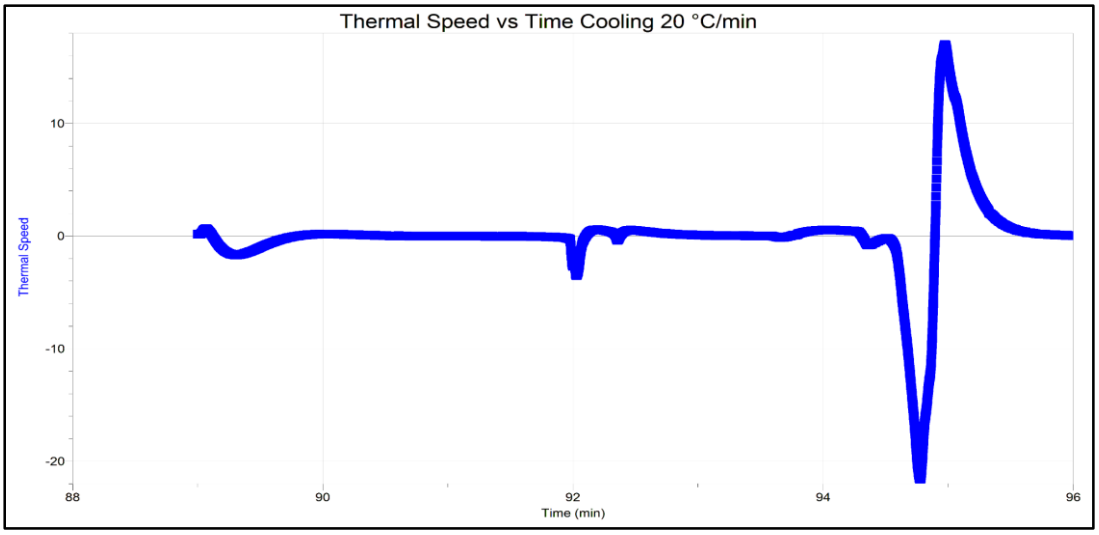

Figure 32: Thermal Speed vs time graph for 8CB liquid crystal while it is cooling in DSC with 20 °C/min rate.

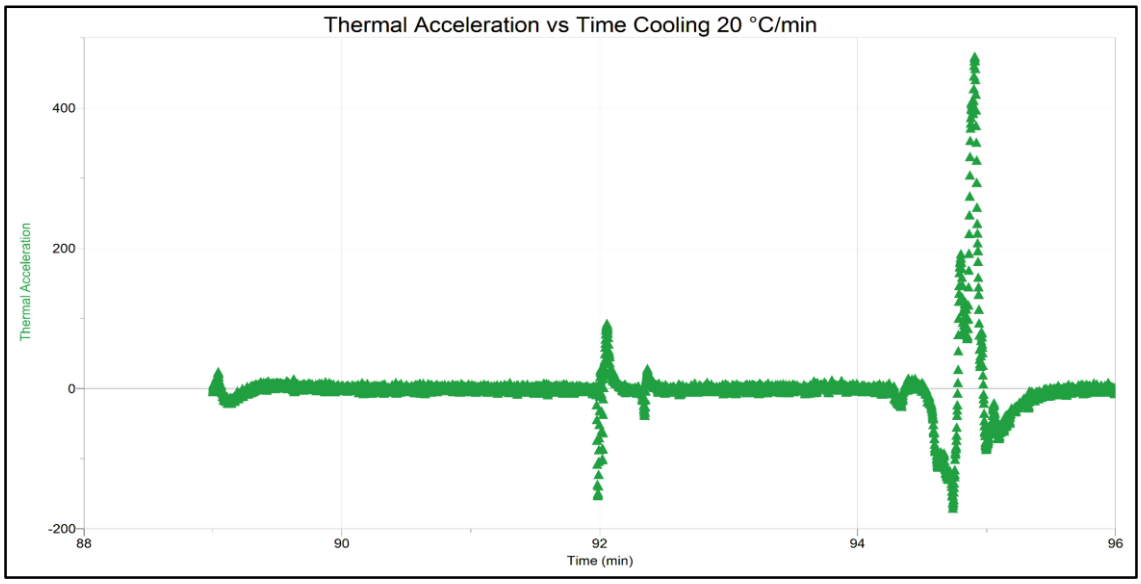

Figure 33: Thermal acceleration vs time graph for 8CB liquid crystal while it is cooling in DSC with 20 °C/min rate.

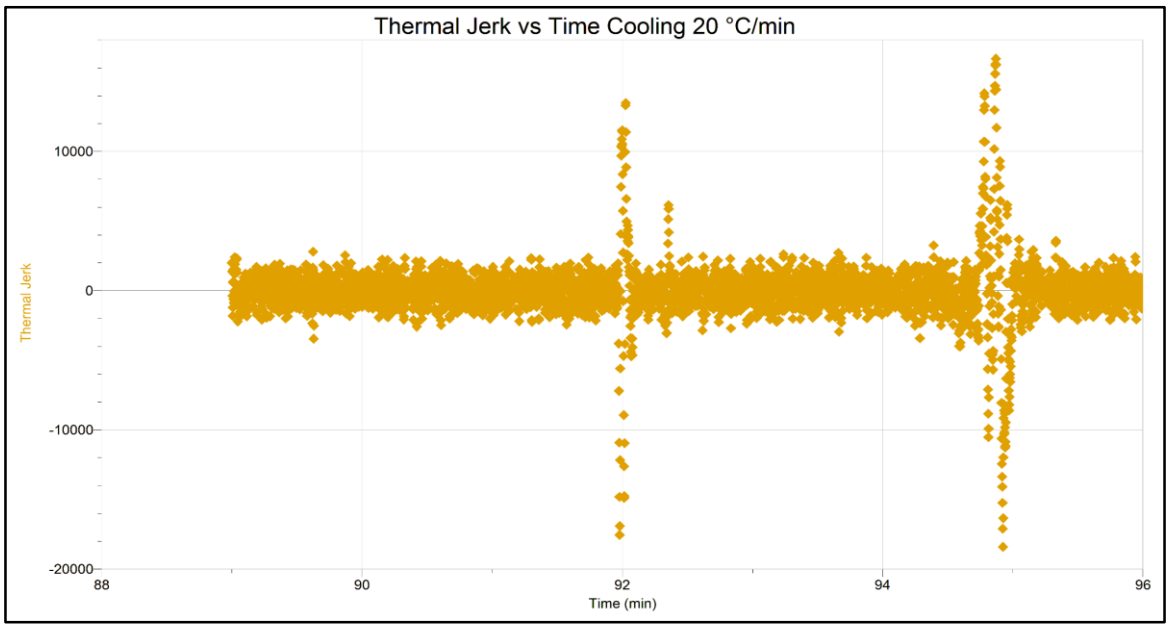

Figure 34: Thermal jerk vs time graph for 8CB liquid crystal while it is cooling in DSC with 20 °C/min rate.

Figures 30-34 depict the data collected for segment 2 (0°C/20.0(K/min)/100°C). **Figure 30** provides a comparison between temperature and heat flow for the phase peak, with detailed data available in **Table 1.** In **Figure 31**, the heat flow and time during the cooling of 8CB LC are presented, featuring peaks for crystalline (k), smectic (sm), and nematic (n) phases. **Figures 32-34** offer comparisons of heat flow and time, utilizing quantitative representations of thermal speed, acceleration, and jerk. **Equations 4-6** were employed to create these derived graphical representations using LoggerPro. The peak values for the derivative graphs are recorded in **Table 7.** The overall thermal speed, acceleration, and jerk exhibit a trend of intensification and faster transitions compared to the heat flow rates of 5.0 (K/min) and 10.0(K/min). It is noteworthy that while the cooling derivatives did accelerate, they generally spanned longer periods than their heating counterparts, on average.

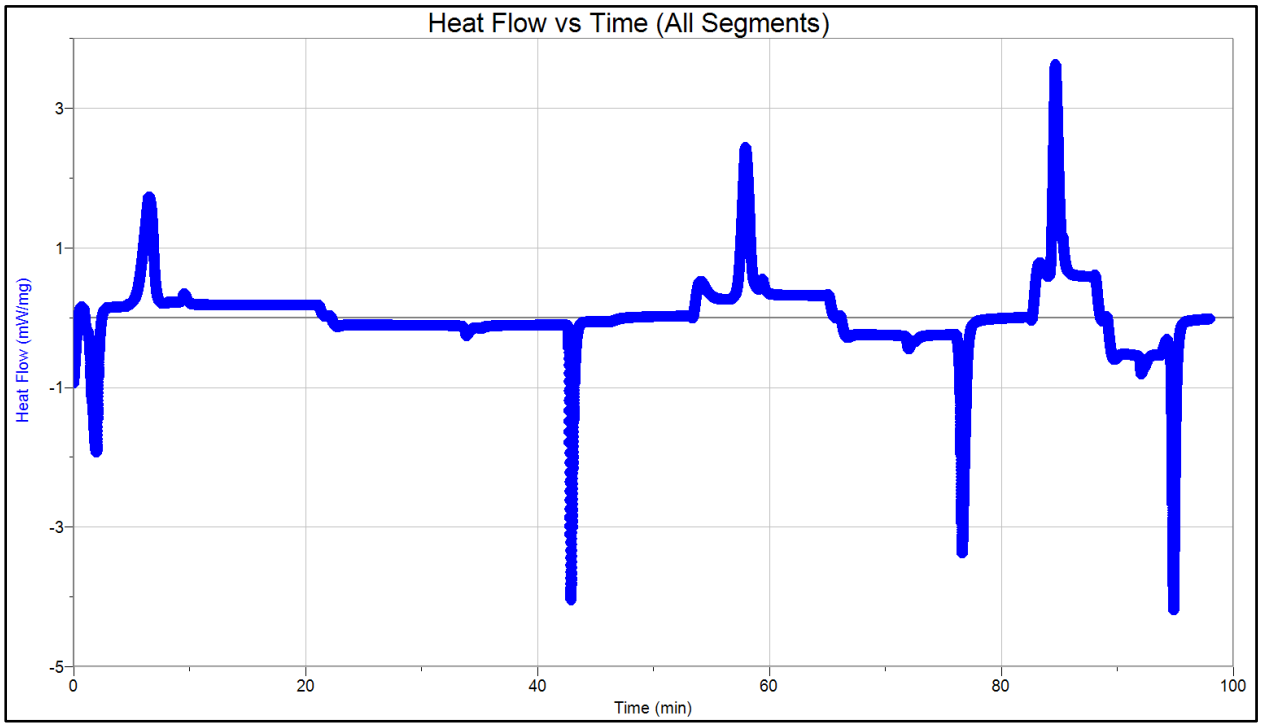

Figure 35: Thermal jerk vs time graph for 8CB liquid crystal using whole data set

Figure 35 presents a visualization of the time and heat flow of 8CB throughout the entire DSC run, encompassing three ramp rates of 5.0, 10.0, and 20.0 (°C/min). The graph showcases a noticeable compression of the time frame in which the peaks occur, corresponding to the increased ramp rates, along with some heightened peaks in the phase transition. The breakdown of individual segments can be observed in **Figures 6, 11, 16, 21, 26, and 31.** The temperatures corresponding to the peaks are documented in **Tables 1-7.** Additionally, this graph highlights a phenomenon visible in more detail in **Figures 3 and 4:** just before the start of ramp rates 10.0 and 20.0(K/min), there is a slight step observed right before the isothermal segments (approximately 43 and 80 minutes into the run).

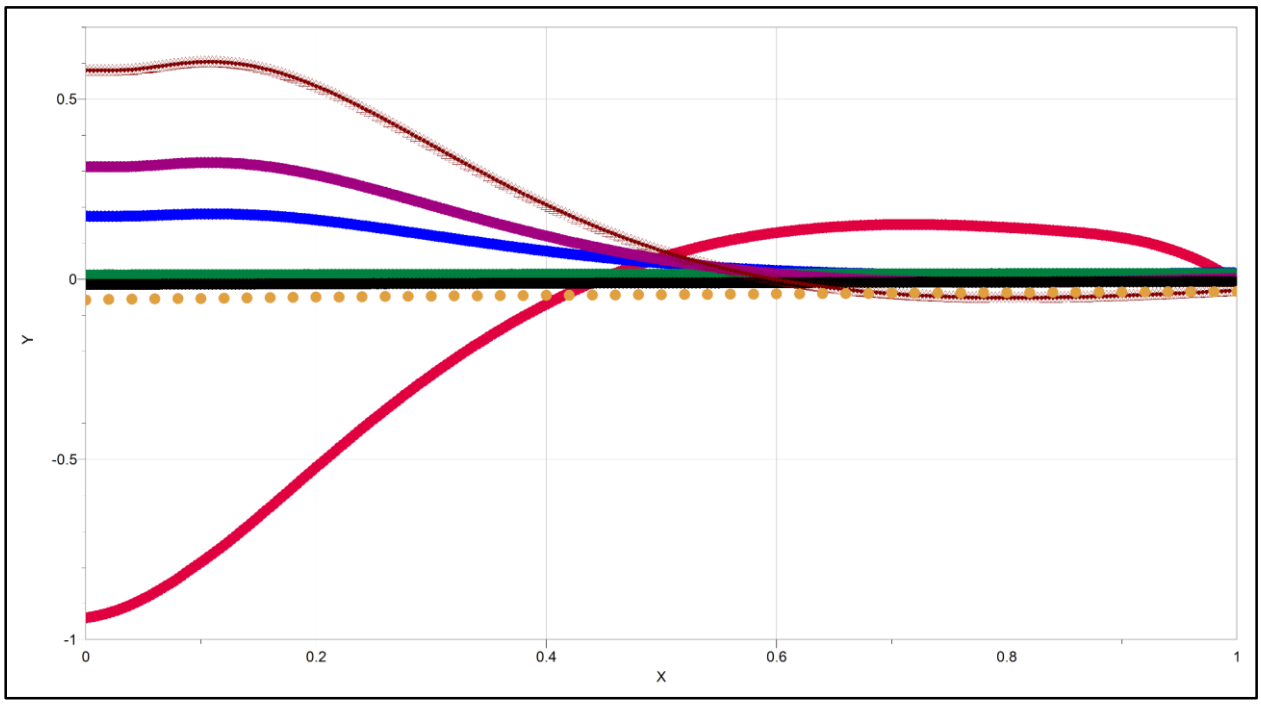

Figure 36: Heat flow (W/g on Y axis) vs. Time (s on X axis) for segments 1, 3, 5, 7, 9, 11, 13.

DISCUSSION

In this discussion section, we will mainly focus on the ranges observed for the heating and cooling processes, highlighting the dynamic nature of the sample under study. The ranges for heating and cooling are determined by subtracting the highest temperature from the lowest temperature achieved during these processes, providing insights into the transitional phases experienced by the material. In this study, the lowest temperature was -40 °C and the highest was 100 °C, resulting in a 140 °C range overall. Our research focuses on 8CB, an intermediate-sized molecule within the family of LC compounds that also includes 4CB and 6CB, which are each characterized by distinct phase transitions. Further information into the characteristics found in 8CB and other liquid crystals in its family can be found in Juliana, Laura, and Kris' papers [16-18]. 8CB demonstrates phase transitions at higher temperatures, notably featuring a smectic A state—a distinguishing trait not observed in lighter LC compounds such as 4CB.

Utilizing Differential Scanning Calorimetry (DSC), our data reveals the precise temperatures at which these phase transitions occur. Notably, when subjected to cooling at different rates, the peak transition temperatures exhibit the trend of moving towards lower temperatures as the rate increases. Conversely, heating moves the phase changes toward higher temperatures as the rate increases, elucidating the dynamic response of 8CB to thermal stimuli as shown in **Table 1.** Unlike its more stable counterpart, 8OCB, 8CB exhibits dynamic behavior, as evidenced by fluctuating phase transitions influenced by both time and temperature. The addition of an oxygen atom at the start of the tail of 8OCB compared to its nonexistence in 8CB enhances the molecule's rigidity by introducing steric hindrance, limiting rotation around the carbon-oxygen bond. In addition, the polarity of the C-O bond in 8OCB can lead to specific intermolecular interactions, further stabilizing the molecular structure. These two factors are the cause of why 8OCB has increased rigidity compared to 8CB, and thus why 8CB is considered dynamic while 8OCB is not. [19] Due to these reasons, keeping 8CB at a specific temperature unveils varying heat flow behavior, indicative of its dynamic nature. The observed fluctuations in heat flow, depicted in **Figure 36**, underscore the material's propensity for dynamic responses to changing thermal conditions.

Despite its dynamic behavior, 8CB remains a widely utilized liquid crystal due to its popularity, ease of manufacture, and versatility in research applications. Its dynamic nature can also be used in its favor, as the versatility and responsiveness of the material is much more sensitive compared to other liquid crystals. Its phase transition rates, both smectic and nematic, exhibit variation, further emphasizing its dynamic nature. Affordable and readily available, 8CB finds extensive use across various technological fields, owing to its well-understood properties and broad applicability.

CONCLUSION

Further examination of liquid crystals was conducted in detail using Differential Scanning Calorimetry (DSC), coupled with an analysis of mesophases using LoggerPro to determine their distinctive properties. Through this comprehensive approach, each mesophase revealed alterations in its characteristics when subjected to varying rates of heating or cooling. The implications of this research extend far beyond the confines of the laboratory and can help assist in increasing its practical

applications, particularly in the development of smart devices. A deeper understanding of liquid crystal behavior afforded by this study both enriches academic knowledge and adds to an already well-researched topic, but also offers practical benefits to industries reliant on such materials. By systematically dissecting the effects of temperature changes on liquid crystals, this study provides more data and research for optimizing 8CB's performance, functionality, and efficiency in various technological applications such as displays, sensors, or optoelectronic devices.

As smart devices continue to become more advanced and capable, the demand for innovative materials that can meet evolving technological needs grows ever more pressing. In this context, the knowledge gained by this research serves to create a better understanding of the advancement of liquid crystal technology, driving forward the development of next-generation devices with improved reliability, responsiveness, and versatility using this dynamic material. This study helps improve our fundamental understanding of liquid crystals and also has the effect of catalyzing advancements that have the potential to reshape the landscape of modern technology, ultimately benefiting society at large.

REFERENCES

1. Seide, M., Doran, M. C., & Sharma, D. (2022). Analyzing Nematic to Isotropic (N-I) Phase Transition of nCB Liquid Crystals using Logger Pro. European Journal of Applied Sciences, 10(3). 98-124.
2. Medaelle Seide, Dipti Sharma, "Reporting Phase Transitions of a New Generation "Tertiary Liquid Crystal System" (TLCS) using Logger Pro," *SSRG International Journal of Applied Physics*, vol. 10, no. 1, pp. 1-5, 2023. *Crossref*, https://doi.org/10.14445/23500301/IJAP-V10I1P104
3. Shen, Y.; Dierking, I. Perspectives in Liquid-Crystal-Aided Nanotechnology and Nanoscience. *Appl. Sci.* 2019, *9*, 2512. https://doi.org/10.3390/app9122512
4. Libretexts. (2023, January 30). *Phase diagrams*. Chemistry LibreTexts. https://chem.libretexts.org/Bookshelves/Physical_and_Theoretical_Chemistry_Textbook_Maps/Supplemental_Modules_(Physical_and_Theoretical_Chemistry)/Physical_Properties_of_Matter/States_of_Matter/Phase_Transitions/Phase_Diagrams
5. Freire, E., Freyer, M. W., Haq, I., Huang, C., Husler, P. L., Lobo, B. A., Makhatadze, G. I., Makube, N., Mason, J. T., McElhaney, R. N., Plotnikov, V. V., Plum, G. E., Privalov, G., Ali, S., Chalikian, T. V., & Cooper, A. (2007, October 26). Differential scanning calorimetry. Methods in Cell Biology. https://www.sciencedirect.com/science/article/abs/pii/S0091679X07840052
6. Schadt, M. How we made the liquid crystal display. Nat Electron 1, 481 (2018). https://doi.org/10.1038/s41928-018-0119-8
7. Krishna Bisoyi, H., & Kumar, S. (2009, September 23). Discotic Nematic Liquid Crystals: Science and Technology. Chemical Society Reviews. https://pubs.rsc.org/en/content/articlehtml/2010/cs/b901792p, 10.1039/B901792P.
8. National Center for Biotechnology Information (2024). PubChem Compound Summary for CID 104289, 4-Cyano-4'-octylbiphenyl. Retrieved March 29, 2024 from https://pubchem.ncbi.nlm.nih.gov/compound/4-Cyano-4_-octylbiphenyl.
9. Schadt, M. (1997, August 1). Liquid crystal materials and liquid crystal displays. Annual Review of Materials Research. https://www.annualreviews.org/content/journals/10.1146/annurev.matsci.27.1.305
10. Özgan, Ş., Okumuş, M. Thermal and Spectrophotometric Analysis of Liquid Crystal 8CB/8OCB Mixtures. Braz J Phys 41, 118–122 (2011). https://doi.org/10.1007/s13538-011-0034-1
11. Devadiga, D., Tan, L. N., Luk, Y. Y., Hu, Q.-Z., Ma, H., Li, G., Wang, Y., Hu, Q. Z., Buyuktanir, E. A., Munir, S., Duan, R., Rouhbakhsh, Z., Yin, F., Liu, J., Baetens, R., Tarantini, M., Aldawoud, A., Dussault, J.-M., Yi, Y. K., … Lockwood, N. A. (2021, November 17). A review on the emerging applications of 4-Cyano-4′-alkylbiphenyl (NCB) liquid crystals beyond display. Materials Science and Engineering: B. https://www.sciencedirect.com/science/article/pii/S0921510721004773
12. Poole, P. L., Andereck, C. D., Schumacher, D. W., Daskalova, R. L., Feister, S., George, K. M., Willis, C., Akli, K. U., & Chowdhury, E. A. (2014, June 26). *Liquid crystal films as on-demand, variable thickness (50–5000 nm) targets for intense lasers*. AIP Publishing. https://doi.org/10.1063/1.4885100
13. *Logger pro® 3 demo*. Vernier. (2023, January 18). https://www.vernier.com/downloads/logger-pro-demo/
14. *4 -octyl-4-biphenylcarbonitrile liquid crystal nematic, 98 52709-84-9*. 4 -Octyl-4-biphenylcarbonitrile liquid crystal nematic, 98 52709-84-9. (n.d.). https://www.sigmaaldrich.com/US/en/product/aldrich/338680
15. Mattia Felice Palermo, Antonio Pizzirusso, Luca Muccioli, Claudio Zannoni; An atomistic description of the nematic and smectic phases of 4-

n-octyl-4′ cyanobiphenyl (8CB). *J. Chem. Phys.* 28 May 2013; 138 (20): 204901. https://doi.org/10.1063/1.4804270

16. McDonough, K., Vy, N. C., & Sharma, D. (2014, April 22). *Existence of time lag in crystalline to smectic A (K–SMA) phase transition of 4-decyl-4-biphenylcarbonitrile (10CB) liquid crystal - journal of thermal analysis and Calorimetry*. SpringerLink. https://link.springer.com/article/10.1007/s10973-014-3812-5
17. Byrne, L. E., & Sharma, D. D. (2023). *Effect of Heating and Cooling on 6CB Liquid Crystal Using DSC Technique. Engineering And Technology Journal*, 8(9), 2740–2756. https://doi.org/10.47191/etj/v8i9.04
18. Mello, J. (2022). Details of Nematic Phase Transition and Nematic Range of 5OCB Liquid Crystal using Logger Pro. *International Journal of Research in Engineering and Science*, *10*(9), 197–217.https://www.ijres.org/papers/Volume-10/Issue-9/1009197217.pdf
19. Ghosh, S., & Roy, A. (2021). Crystal polymorphism of 8ocb liquid crystal consisting of strongly polar rod-like molecules. *RSC Advances*, *11*(9), 4958–4965. https://doi.org/10.1039/d0ra08543j